UNIVERSITY OF CAPE TOWN

FACULTY OF ENGINEERING AND THE BUILT ENVIRONMENT

DEPARTMENT OF ELECTRICAL ENGINNERING

MSc (Eng) Dissertation

Estimation of Geomagnetically Induced Currents (GICs) in the Namibian Transmission network

Prepared by: Magnaem Ngendina Simon

Supervisor: Professor C.T. Gaunt

Declaration

I understand the meaning of plagiarism and I declare that all the work presented in this dissertation is my own, save for that which is property is acknowledged. This dissertation is being submitted in fulfilment of the degree of Master of Science in Engineering in the University of Cape Town and has not been submitted before for any degree or examination.

November 2013

Abstract

Geomagnetically Induced Currents (GICs) have become a matter of concern not only to networks located in high magnetic latitude regions but also in networks located in mid-latitude regions. GICs pose a threat of transmission equipment damage which could lead to short power interruptions and potentially long term blackouts. Improved modelling techniques are essential in predicting the GICs flowing in the network in order to enable power utilities to reduce the risk of damage to equipment and improve the reliability of their power supply.

This dissertation, entitled *ESTIMATION OF GEOMAGNETICALLY INDUCED CURRENTS (GICS) IN THE NAMIBIAN TRANSMISSION NETWORK,* aims at improving GIC estimation by installing measurement equipment in order to compare measured GIC results with modelled results. The purpose of which is to validate the calculation technique. The Nodal Admittance technique was proposed for the study and was first validated using published data obtained using the *a&b* parameter method. For the measurement techniques, two methods were found namely direct measurements in the transformer neutral conductor and indirect measurements in the transmission lines. In this dissertation, the former was implemented due to its simplicity in usage.

A direct measurement approach was chosen and the criteria for choosing the measurement devices were discussed. The complete measurement set-up was first tested in the laboratory on a published laboratory set-up before it was installed in the network. Two substations were chosen for GIC monitoring namely Ruacana and Obib substation. Thereafter the equipment was installed at the two substations on three transformers, one at Obib and two at Ruacana substation, to measure GICs in the network during solar storms. Comparisons of measured and modelled results were performed, obtained using the Nodal Admittance technique, to investigate how closely the measured and modelled results correlate. Findings showed that results for geomagnetically quiet days appeared to be temperature dependent. After applying a temperature compensation technique on the geomagnetically storm day's results, it was found that the measurements respond similar to what was expected from the calculations. From the calculation technique, Ruacana substation was found to have the highest GIC in the network.

Acknowledgements

First and foremost I would like to thank God for the opportunity of education, for the strength, grace and wisdom He has bestowed on me during this time. Without God none of this could have been possible.

I would also like to thank my supervisor Professor C.T. Gaunt for all the assistance and supervision during the course of my research. His guidance and support carried me till the end.

I thank NamPower for all the financial assistance throughout my university studies. Words cannot express how grateful I am for trusting me and believing in me. I cannot forget to mention all the NamPower personnel who assisted me during my research, but to mention a few, I would like to thank Mr Frank Engelbrecht, Mr David Magongo, Mr Helgo Muller, Gernot Heger, Patric Molebugi, Lionel Kuzatjike and everyone who I have consulted with. Your assistance was invaluable and I thank you all for your patience and motivation.

Last but not least, I would like to thank my family and friends, thank you for all your prayers and encouragements. You have been a rock for me during my entire research, I could not have asked for more. Thank you to Saari Simon for always making me laugh.

Table of Contents

List of figures

List of tables

Chapter 1

Introduction

This chapter introduces a brief overview of Geomagnetically Induced Currents (GICs), their causes and effects on power systems. It then proceeds to cover the objectives and motivation for this dissertation. Furthermore, research questions are also presented with an aim to test the hypothesis identified in this chapter. In addition, the methodology employed in the dissertation is also discussed.

1.1 Overview of Geomagnetically Induced Currents

The purpose of this dissertation is to investigate calculation and measurement techniques suitable for the study of Geomagnetically Induced Current (GIC) in the Namibian transmission network, and to thereafter compare measured results with calculated results. GICs are a "quasi" direct current with frequencies ranging from 0.1 mHz to 10 mHz which enter the transmission network via transformer neutral conductors and are reported to have contributed to equipment damages in power networks mainly transformers [Kappenman & Albertson, 1990].

As the world's demand for energy increases, the pressure on suppliers is enormous. Meeting the energy demand is challenged by various factors which affect the reliability of power systems, including lightning, animals, fires, and adverse weather conditions [Department of Public Utilities, 2008]. Of late, GICs which are caused as a result of solar events have also been suggested to affect power system reliability [Kappenman & Albertson, 1990].

There are three main solar events namely solar flares, coronal holes and disappearing filaments. During an event known as coronal mass ejection (CME), the sun emits large masses of charged particles and this phenomenon is called the solar wind [IEEE working group, 1993]. These large masses of charged particles are sometimes released towards the earth's surface - a process called Geomagnetic Disturbances (GMDs) [IEEE working group, 1993]. The interaction between these charged particles and the Earth's magnetic field causes fluctuations of the magnetic field, which then induces currents in the ground known as GICs [IEEE working group, 1993].

GMDs tend to follow approximately an 11 year cycle [IEEE working group, 1993]. The current solar cycle is cycle 24 which commenced in December 2008 and the solar maximum of this cycle is estimated to occur in 2013. The “solar maximum“ is the period when there is more activity on the sun’s surface whereas the “solar minimum” is the period when there is least activity on the sun’s surface in any particular cycle [IEEE working group, 1993; Kappenman & Albertson, 1990]. In general, GMDs tend to occur during solar maximums although they may also take place at any time during the cycle.

GICs have been observed to cause transformers to operate under half-cycle saturation; consequently, this may lead to an increase in non-active power consumption and increased harmonics which may lead to transformer failure - thereby compromising the reliability of the power system [Molinski, 2002; Amuanyena & Gaunt, 2003]. Laboratory experiments carrying out the effects of GICs on transformers have been reported [Kappenman & Albertson, 1990; Molinski, 2002; Girgis & Gramm, 2012; Ngnegueu et al., 2012; Bachinger et al., 2012]. Pinto et al. [2005] also reported that some types of digital relays are more sensitive to harmonics. In the presence of harmonics, these relays may be improperly triggered, hence disrupting the protection system actions [IEEE working group, 1993].

To be able to combat the effects of GICs in power systems, mitigation techniques have been developed. However, GIC mitigation techniques are outside the scope of this thesis. Nonetheless it is important to note that several techniques exist for GIC mitigation and some are discussed briefly herein. These include: GIC blocking devices, neutral-to-ground resistors, transformer shut down and space weather monitoring [Prabhakara et al., 1992]. The technique of GIC blocking devices has been used by the Hydro-Quebec utility in some of their High Voltage (HV) lines [Molinski, 2002]. GIC mitigation techniques should be used with caution to avoid the possibility of distributing GIC flow to other parts of the network, which may lead to more damage [Pirjola, 2002].

1.2 GIC occurrences and research specifications

Canada and the Scandinavian countries, situated at high magnetic latitude regions, are more prone to high GICs [Kappenman & Albertson, 1990]. However, networks situated in mid-latitude regions, such as the Southern African network, are also susceptible to GICs although their magnitudes may be smaller in comparison to those at high latitude [Koen, 2002; Koen & Gaunt, 2002; Koen & Gaunt, 2003]. The Southern African network consist of long transmission lines and the use of larger power transformers which are reported to be

one of the reasons why today's power systems more susceptible to GICs [Amuanyena & Gaunt, 2003].

Two major magnetic storms that have been reported are the Quebec storm [Kappenman & Albertson, 1990] which took place in March 1989 and the Halloween storm which took place in October 2003 [Pirjola et al, 2010]. Both of these solar storms resulted in numerous equipment damages and several mal-functions of relays.

The Namibian power (NamPower) utility felt it was important to examine and determine how vulnerable their transmission network is to GICs. Therefore, the focus of this study is to investigate modelling and measurement techniques suitable for the Namibian network.

Research motivation

Effects of GICs on the NamPower network have not been previously measured. It is therefore essential for NamPower to evaluate their network's susceptibility to GICs in order to determine how this influences both their short-term and long-term planning. This may help minimise equipment losses and enable the utility to improve power system reliability.

The specific objectives of this dissertation are therefore to:

- Investigate and determine what chosen GIC measurement techniques are suitable for the Namibian transmission network
- Suggest appropriate equipment and installation thereof to measure GICs
- Investigate and determine what modelling techniques are suitable for the Namibian transmission network and calculating GICs flowing in the network.
- Compare modelled and measured results in order to validate the modelling technique used.
- Comment on the exposure of the Namibian transmission network to GICs based on the modelled results.

1.3 Hypothesis to be investigated

The topology of the NamPower transmission network consists of long transmission lines and few nodes.

Several techniques have been developed to calculate GIC magnitudes in power networks. Input parameters to be used in the GIC modelling techniques should be very carefully chosen to ensure that the modelled results are consistent with measured data. The inputs to these models include network parameters, electric field data and the ground conductivity of the network, while the output is a GIC magnitude at each point in the network.

The hypothesis to be investigated in this dissertation is, therefore:

Advanced network modelling algorithms can be used efficiently together with measurement results, to predict the flow of GICs in the Namibian transmission network.

The research questions needed to test the validity of the above hypothesis include:

- What is the appropriate ground conductivity for Namibia to be used in the models?
- What analytical or simulation techniques are available for GIC study?
- What parameters are required for the modelling techniques and are they available?
- How will GIC measurements be done?
- How accurate are the algorithms results in comparison with measurements?
- What is the exposure of the Namibian network to GICs?

1.4 Methodology

The activities shown below are the main actions that were carried out in this study in an attempt to answer the research questions outlined in section 1.3.

Literature review

This chapter aims to answer the research questions stated in chapter one based on the available literature. It begins with reviewing existing ground conductivity models and various assumptions made in these models in previous studies. In addition, it also includes correlations between simulated versus measured results using different conductivity models. Thereafter, electric field modelling techniques available for GIC studies are covered which includes the plane wave method, the Complex Image Method (CIM) and the Spherical Elementary Current Systems (SECS) method. Finally, different GIC measurement

techniques are discussed and the exposure of the Namibian network to GIC is reviewed based on previous solar storms as published.

Theory development

Having reviewed several techniques for calculating GICs in chapter two, this chapter will give more details and derivations on the plane wave method and the SECS method. Assumptions made and equations used in the two methods to model the electric field will also be covered. Thereafter, two methods for GIC calculations namely the *a&b* parameter and the Nodal Admittance method will be discussed including the assumptions made for each method. Furthermore, two different measurement techniques for GICs in the network will be discussed as well as the challenges associated with the implementation of these measurement techniques.

Test network

Before adopting the Nodal Admittance method to the Namibian network, a simple application of the technique was done on simple circuits. Thereafter, the network used in the previous study done on the Namibian network will be used as a test system using the *a&b* parameter method. The Nodal Admittance method will be applied on the same test system used by the *a&b* parameter method to calculate GICs on the test network and the results will be compared to those obtained previously using the *a&b* parameter method. This analysis will be done under similar test conditions and will serve as a first validation process for the Nodal Admittance method.

Measurement and monitoring assessment

In this chapter, the proposed measurement technique for this dissertation suggested in the theory development chapter will be discussed. Description of the process of choosing measuring equipment used in this dissertation will also be presented. All procedures followed to determine the choice of the equipment will be shown, including equipment specifications. Furthermore, proposed substations to be adopted for GIC measurements will be identified and the installation procedure followed will be discussed. A laboratory prototype used to test the measurement equipment will also be described.

GIC measurements in the Namibian transmission network

In this chapter, preliminary measured results are discussed and compared to what was expected. Measurements taken for geomagnetically quiet days and geomagnetically storm days are shown and discussed.

After validating the Nodal Admittance technique using previously published data, the Nodal Admittance method will be used to calculate GIC on the current network. Subsequently, correlations with the measured and the modelled results will be assessed. Any further observation depicted from the data is also covered in this chapter.

Conclusion

This section summarizes the findings from Chapter 6 It also highlights the main findings covered in previous chapters

Chapter 2

Literature review on Geomagnetically Induced Currents

This chapter aims to answer the research questions stated in section 1.3 in an attempt to test the proposed hypothesis. Different modelling and measurement techniques used in this dissertation and the expected results are discussed in this chapter. Characteristics which make the Namibian transmission network susceptible to GICs will also be presented in this chapter.

2.1 Exposure of the Namibian transmission network to GICs

GICs are quasi-DC currents caused as a result of fluctuations of the earth magnetic field interacting with charged particles from the sun through a phenomenon called the solar wind [IEEE working group, 1993]. Solar activities tend to follow an 11 year cycle. The next peak (cycle 24) is expected to occur in 2013.

In this section, factors influencing network susceptibility to GICs are covered. Also, previous GIC results obtained for the Namibian network and South African network will be summarized.

Characteristics of the network that influence GIC intensity

GIC magnitudes and their effects on the transmission network are influenced by several factors. These factors can be divided into two categories, namely; characteristics of horizontal electric fields of a power system and network characteristics [Molinski, 2002]:

A. Characteristics of horizontal electric fields in power systems. This depends on the following:

- Ionospheric currents which depends on time and space
- Earth's conductivity which depends on time and space
- Location of the power system with respect to the auroral zone

B. Network characteristics. These depend on the following:

- Orientation of the power lines (i.e., north-southerly versus east-westerly)
- Lengths of transmission lines
- Resistance of the electrical systems (transmission lines)
- Resistance and configuration of transformer windings
- Grounding of the substation
- Type and connection of transformer

These factors influence the extent of susceptibility of different areas in the same network or at the same magnetic latitude. It has been reported that networks in areas closer to the aurora zones tend to be more susceptible to high GICs. Furthermore, coastal regions appear to be prone to high GIC levels. This is due to the fact that there is high ground resistance at the regions where the ocean meets the land - thereby causing GICs to seek other alternative routes such as network equipment [IEEE Working Group, 1993].

The Southern African transmission network comprises of long transmission lines and low ground conductivity. The presence of long transmission lines creates large loops, where even small changes in the earth's magnetic field may induce large GIC magnitudes [Koen, 2002; Koen& Gaunt, 2003; Kappenman & Albertson, 1990] as portrayed in **Figure 2-1.**

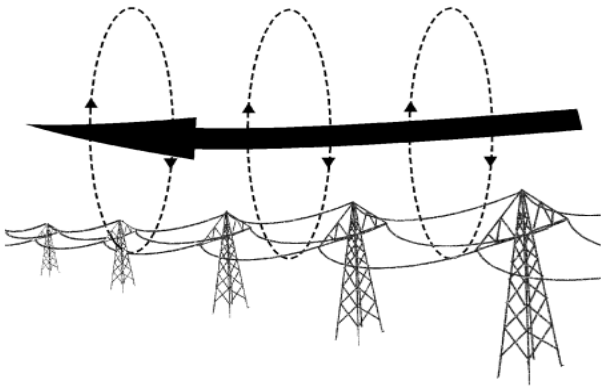

Figure 2-1: GIC induction in long transmission lines [Boteler, 2003]

Table 2-1 shows GIC results for the NamPower transmission network obtained from Koen [2002] using 13th March 1989 storm data where *a&b* are the system parameters.

Table 2-1: GIC magnitudes for the Namibian network [Koen, 2002]

Substation	a-Value	b-Value	GIC max [A]
Oranjemond	26	-19	-18
Gromis	-23	-17	7
Nama	-21	-7	6
Aggeneis	-25	-14	7
Aries	-85	116	63
Kokerboom	-25	-24	9
Auas	54	-6	-22
Van Eck	33	12	-9
Omburu	3	-16	-5
Ruacana	63	-26	-30

Table 2-2 shows a list of substations in the South African network which are most susceptible to GICs.

Table 2-2: Substations most susceptible to GICs in South Africa obtained from Koen& Gaunt [2003]

Substation	Maximum calculated GIC on 13 March 1989 averaged over 1 minute (A)
Alpha	108
Hydra	67
Beta	64
Grootvlei	59
Perseus	57
Grassridge	41

Transformers at base load power stations appear to be more vulnerable to GICs since they are relatively more heavily loaded than transformers located further away from the base load power stations. This is because they are normally operated close to their rated values [Gaunt & Coetzee, 2007].

It has been reported that substations situated at the ends and at the corners of long transmission lines are prone to maximum GIC magnitudes [Boteler et al., 1994; Pirjola & Boteler, 2006; Pirjola et al., 2010]. These are the substations which are only connected to one substation on one end and a transmission line on the other end. This finding was deduced from a study done using data from the Canadian Hydro-Quebec system, assuming uniform electric field and constant ground conductivity over the entire network [Boteler et al., 1994].

Large GIC magnitudes were found in areas with east-westerly transmission lines [Pirjola, 2002; Breckenridge et al., 2001]. However, this study was done in a region close to the auroral zone and may not necessarily agree with regions far from the auroral zone. An investigation was done on the Namibian network and reported that south-northerly lines appeared to be more susceptible to GICs than the east-westerly lines [Zatjirua, 2005]. This finding was also reported by Liu et al. [2009] for the Japanese network.

The level of geomagnetic activity can be indicated using various indices. For the purpose of this dissertation, only the A_k and K_p indices are discussed. The K_p index ranges from 0 to 9, representing the peak geomagnetic activity over a 3 hour period. The K_p index referred to in this dissertation refers to the planetary K_p index. The A_k index is a linear index, derived from the logarithmic K_p values, ranging from 0-400 [Molinski, 2002]. Kappenman & Albertson [1990] reported that K_p index greater than 5 is caused by solar storms of high intensity. Kappenman & Albertson [1990] also stated that the solar storm that resulted in a blackout of the Canadian Hydro-Quebec region corresponded to an index of K_p =9. A_k and K_p values are measured daily at the Magnetic Observatories. **Table 2-3** shows corresponding A_k values for the given K (HER) values obtained from Koen [2002] measured at the Hermanus Magnetic Observatory.

Table 2-3: Correlation of the A amplitude for the corresponding K_p -index [Koen, 2002]

K_p	0	1	2	3	4	5	6	7	8	9
A_k	0	3	7	15	27	48	80	140	240	400

Ngwira et al. [2011] argued that using the K_p -index to classify the intensity of geomagnetic activity is not sufficient, since the K_p -index does not provide adequate measurement of the level of geomagnetic activity in nano-Tesla (nT). Ngwira et al. [2011] stressed that there is a need to evaluate current parameters to find the ones that best classify the severity of

geomagnetic storms. In the same paper [Ngwira et al., 2011], the results obtained showed that there are very poor correlation between the geomagnetic field (B-field) and GICs, but peak |*d*B/*d*t| shows a good correlation to peak GICs. However, Watari [2009] reported that in Japan, there appear to be better correlation to the deviation in the geomagnetic horizontal B-field than to *d*B/*d*t with GICs.

2.2 Exposure of the Namibian network to GICs

One of the research questions is to investigate the exposure of the Namibian transmission network to GICs. This will be looked at in this section from previous solar storms.

There have been fault incidents reported on the Namibian network which took place during some of the previous magnetic storms reported. In this section, some of the incidents reported are discussed.

On the 11 December 2003, a 90 MVA, 330 kV, two-year old transformer at the Ruacana substation tripped. It was found that, the master relay trip was caused by Buccholz and differential protection [Zatjirua, 2005; Gaunt & Coetzee, 2007]. **Table 2-4** shows faults experienced by transformers at the Ruacana power station and geomagnetic events which took place during the same period from October 2003 to November 2004. **Table 2-4** was published by Zatjirua [2005] however the original report from NamPower was never published but only referenced by Zatjirua [2005].

Table 2-4: Faults and geomagnetic events at Ruacana power station [Zatjirua, 2005]

DATE OF STORM	K-INDEX	DATE OF EVENT	POWER SYSTEM EVENT
October 29-31, 2003	K>6	October 30, 2003	Generator 1 at Ruacana tripped: low tank pressure
November 20-21, 2003	K>6	December 11, 2003	Generator 2 at Ruacana tripped: Buccholz alarm and overall trip, emergency declared
July 23-28, 2004	K>6	July 28, 2004	Generators 1, 2 and 3 at Ruacana tripped: emergency declared
November 8-10, 2004	K>6	November 18, 2004	Generators 1, 2 and 3 tripped: emergency declared

Table 2-4, show that only K-indices above K-5 were reported to cause faults. Four major faults were reported at the Ruacana power station.

The HV winding of the two-year old transformer which was damaged at the Ruacana substation is shown in **Figure 2-2**.

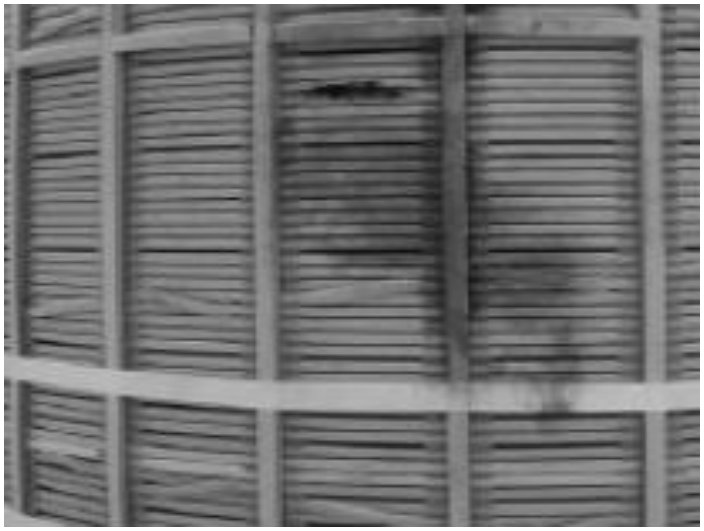

Figure 2-2: Damaged HV winding due to GICs at the Ruacana power station [Gaunt & Coetzee, 2007]

The above incident of the transformer damage at the Ruacana substation initiated GIC study on the Namibian transmission network. Researchers such as Koen [2002] used uniform ground conductivity and fault data obtained from NamPower for GIC calculations from 2003 to 2004, corresponding to solar cycle 23. Zatjirua [2005] later performed a GIC study on the Namibian network using the method applied by Koen [2002] with few modifications. In both studies, the highest GIC magnitudes were reported to be at Ruacana and Aries substations, as they are both located at the ends of the network

It is important to note that, not all transformer failures can be attributed to the presence of GICs. A transformer may also fail months after a major GIC event has taken place. This makes it challenging to attribute all transformer failures to GICs. Furthermore, unless frequent Dissolved Gas Analysis (DGA) is performed, it is difficult to isolate transformer failures which may have taken place as a result of GICs. DGA samples are taken to measure the presence of various gases in the transformer's oil as an indication of possible overheating problems in the transformer [Koen & Gaunt, 2003].

2.3 Ground conductivity models applicable for the Namibian network

Ground conductivity is an important factor necessary to calculate the electric field induced in the ground which leads to an induced GIC. Ground conductivity together with the magnetic field data are used to calculate the electric field. One of the research questions to test the hypothesis for this dissertation is to investigate available ground conductivity models suitable for the Namibian transmission network. In this section, different ground conductivity models will be discussed and comments will be made on their usage and accuracy.

GIC calculation techniques require real time geomagnetic data obtained from magnetic observatories measured using magnetometers. Thereafter, the electric field is calculated from the magnetic field data using the properties of the ground conductivity [Ngwira et al., 2008].

Due to the complexity of ground conductivity properties, previous studies have assumed uniform one dimensional ground conductivity for Southern Africa [Koen, 2002; Zatjirua, 2005; Bernhardi, 2006]. Comparisons of the results obtained from these studies indicate close correlation between measured and modelled results. It should be noted, that although the use of uniform ground conductivity is sufficient to enable utilities to perform quick calculations for analysing GIC magnitudes, it may not be sufficient to give accurate results [Bernhardi, 2006].

To improve the correlation of the measured and modelled results, a three-dimensional conductivity model has been developed by [Ngwira et al. [2008], using GIC measured data from Grassridge substation and geomagnetic data from the Hermanus Magnetic Observatory both in South Africa. The Southern African ground conductivity model was tested using past solar storm data and good correlation was achieved [Ngwira et al. 2009]. However, this model is only valid for GIC data sites close to magnetic observatories. Therefore more magnetometers need to be installed in the network to be able to derive ground conductivity models for each area in the network.

Areas in the Southern African region have different ground conductivities. This means that the three-dimensional ground conductivity model developed by Ngwira et al. [2008] may not necessarily work well with data from sites other than the Hermanus Magnetic Observatory and the Grassridge substation in South Africa. Previously, GIC studies in Namibia were done using uniform ground conductivity models [Koen, 2002; Zatjirua, 2005].To date, very little is known about the ground conductivity in Namibia.

2.4 Techniques developed for electrical field modelling

This section covers one main research question for this dissertation which is to investigate what analytical or simulation techniques are available for GIC study. GIC modelling can be done using a two-step process: firstly, by determining the geo-electric field induced on the ground and secondly, by calculation of GIC magnitudes induced as a result of the induced geo-electric field [Pirjola, 2005]. This section covers methods used to calculate the geo-electric field. These methods differ according to the source current used and the ground conductivity assumed.

Uniform plane wave method

In the plane wave method, the "plane wave" relationship between the electric and magnetic field is assumed. Pirjola states that*, "in the frequency domain, a horizontal electric field component equals the product of the "plane-wave surface impedance", which depends on the earth's (layered) conductivity structure and the perpendicular horizontal magnetic component"* [Pirjola, 2005]. Since the ground conductivity depends on the location of the area, the plane wave method may only be applied locally. The use of uniform plane wave method is sufficient for fast GIC calculations, but may not necessarily yield very accurate results.

Spherical Elementary Current Systems (SECS)

The SECS method uses magnetic field data to derive the ionospheric currents produced. The concept used in SECS is as follows: there exists a horizontal current system for every 3D ionospheric current system which produces the same geomagnetic field at the surface of the earth, even though it is not the real ionospheric current [Bernhardi et al., 2008]. According to Viljanen et al. [2004], using an approximation that neglects ground conductivity and the earth's curvature enables a set of elementary ionospheric currents to be placed in an equally spaced grid. This concept was applied by Bernhardi [2008], who placed an equally spaced grid at a height of 100 km above the Southern African region and calculated the amplitudes of the ionospheric currents by fitting the resultant horizontal geomagnetic field to that measured at various magnetic observatories namely Hermanus, Hartebeesthoek and Tsumeb. Using elementary currents, the horizontal geomagnetic field at any point can then be obtained. The SECS method divides the transmission network into sub-sections and applies the plane wave method to each sub-section. Bernhardi [2008] found that using non-uniform electric field is much more accurate than assuming a uniform field for the entire network.

Complex Image method (CIM)

The Complex Image Method (CIM) is used to calculate electric and magnetic fields produced by an auroral electrojet [Shepherd & Shubitidze, 2003]. The CIM makes use of "image" currents located at complex depths which incorporate the inductive properties of the earth. According to Boteler & Pirjola [1998], the magnetic and electric fields obtained using the CIM method compare well with those obtained using exact computation. It is said that the computation time using CIM is only a small fraction of that required when using exact computation [Shepherd & Shubitidze, 2003]. CIM is restricted to 1 dimension (1D) layered ground conductivity and its accuracy is limited because it depends on the number of computations performed. This method, however, may result in inaccuracies if applied to networks located away from the auroral regions, such as the Southern African networks, because it assumes that the electric and magnetic fields on the earth's surface are caused by auroral electrojet.

2.5 Techniques developed for GIC measurements

Although modelling techniques could be well-suited for predicting GIC magnitudes, it is important that actual GIC measurements be taken in order to verify modelled results. There are two ways to measure GICs, namely, measuring in the transformer neutral conductor and under the transmission lines using magnetometers. These methods are discussed below.

One direct method to measure GICs is to make use of a Hall-Effect transducer to measure GICs that flows in the neutral. This method is found to be easier to implement compared to measuring under the transmission line. It should be noted that measuring GIC magnitudes in the transformer neutral conductor may not give accurate readings especially in cases when there is an autotransformer. This is because, GICs flowing in an autotransformer may not necessarily terminate at a local earthing point because autotransformers have other direct conductive paths to other parts of the network and may contribute to GIC flow in other parts of the network [IEEE working group, 1993; Koen, 2002]. This method was implemented through the Sunburst project, developed by EPRI and used in the United States [Bolduc, 2002] and in England and Whales [Arinmez, 2001]. The EPRI Sunburst was also implemented in South Africa at the Grassridge and Hydra substation [Koen, 2002; Kenny, 2005]. Measured results from Hydra and Grassridge substations showed good correlation with modelled results [Koen, 2002].

The second method is to use magnetometers which can be installed under a transmission line to measure the magnetic field under the line. This method needs to be applied cautiously, since magnetometers are very sensitive to disturbances and therefore measurements should be done in remote areas to minimise disturbances from the surrounding area [Viljanen & Pirjola, 1994].

Other ways that can be implemented for GIC measurements mainly to indicate the level of saturation in the transformers due to GICs, include monitoring the effects of GICs such as transformer temperature rise, harmonics, noise and reactive power [Molinski, 2002]. Koen [2002] found that the presence of the 6^{th} harmonic indicates transformer saturation due to GICs.

2.6 Chapter summary

Factors making the Namibian transmission network vulnerable to GICs were covered which included the presence of long lines, low ground conductivity and the large transformers used to enable the utility to transmit power to many customers located further apart. In this chapter, an attempt was made to answer some of the research questions stated in section 1.3. Various techniques have been developed to model GICs in the transmission networks. Important parameters necessary for GIC modelling were identified and they are: the network parameters, the electric field data and the ground conductivity. These parameters were discussed in detail in relation to the research questions. Lastly, GIC measurement techniques were identified and comments were made on some examples of networks where these techniques were applied.

Chapter 3

Theory Development

In this chapter, the theory development for GIC modelling techniques namely; uniform plane-wave, SECS, the a&b parameter method and the Nodal Admittance method will be covered. Characteristics for the different methods will be discussed and comments will be made on their applications. Thereafter, ways for validating simulation results will be discussed namely; using GIC measurements in the neutral and in the transmission lines.

3.1 Introduction

From Faraday's induction law, variations in the earth's magnetic field will result in a current induced in the ground and thereafter flowing into the transmission network via transformer ground neutrals. Since GICs have a much lower frequency compared to the 50/60 Hz AC network, the transmission network can be simplified to a resistive network.

This chapter addresses GIC modelling techniques which can be done in two parts namely; geophysical calculation and network calculation. The geophysical calculation involves using magnetic field measurements at magnetic observatories, which are then used to calculate the electric field induced in the ground. Subsequently, the network calculations are performed using the electric field induced in the network to calculate GICs at every point in the network.

3.2 Geophysical calculation

In the geophysical calculation step, the methods used to calculate electric field differ by the assumptions made about the source current and the ground conductivity. Below are the different methods used to calculate the electric field:

Plane-wave method

The plane-wave method ignores the curvature of the earth's surface. By ignoring the curvature, a Cartesian coordinate system can be established where x, y and z coordinates are chosen to point northward, eastward and downward respectively. The electric and magnetic fields induced by source currents can be assumed to be plane-waves propagating parallel to the x axis while the ground conductivity is assumed to be uniform.

A relationship between the magnetic field and the electric fields exist as follow [Viljanen & Pirjola, 1989]:

$$E(t) = -\frac{1}{\sqrt{\pi\mu_0\sigma}}\int_{\infty}^{t}\frac{g(u)}{\sqrt{t-u}}du\,, \qquad (1)$$

where $E(t)$ is the y component of the induced electric field, μ_0 is the permeability of free space, σ is the ground conductivity and $g(t)$ is the variation rate of the x component of the magnetic field.

For simplicity, equation (1) can be written as follow to calculate the geoelectric field at a given time T_N:

$$E(T_N) = -\frac{2}{\sqrt{\pi\mu_0\sigma\Delta}}\sum_{n=N-M+1}^{N} b_n(\sqrt{N-n+1}-\sqrt{N-n})\,, \qquad (2)$$

where $b_n = B_n - B_{n-1}$, B_n is the geomagnetic component at time T_n, Δ is the sampling interval, n is the sampling number and M is a number corresponding to how many past magnetic field values should be used to calculate the current electric field

In a previous study by Koen [2002], a value of M =10, σ =0.001 S/m and a 2 minute sampling interval were used together with the magnetic field data from the Hermanus Magnetic Observatory (HMO). The results obtained from this study showed good correlation with measured data from the Grassridge substation in South Africa.

Spherical Elementary Current Systems (SECS)

The SECS method can be broken down into two steps. Firstly, a *model* is built that uses the magnetic field data to derive the equivalent ionospheric currents produced. Thereafter, the electric field at any point in the network can be calculated from the model. In this model, the curvature of the earth's surface and the height of the ionosphere are incorporated unlike in the plane-wave model. The first step assumes that, a horizontal equivalent current system exists for every 3D ionospheric current system. The equivalent current systems reproduce the same geomagnetic field at the earth's surface as the one produced by real ionospheric currents [Pirjola & Viljanen, 1998].

In a previous study by Bernhardi [2006], a set of elementary ionospheric currents were placed in an equally spaced grid, above Southern Africa, at a height of 100 km. The elementary ionospheric current amplitudes were calculated by fitting the resultant horizontal

geomagnetic field from the measured geomagnetic field at different magnetic observatories. In the second step, the horizontal geomagnetic field at any point in the network can be calculated. The SECs method was applied by Bernhardi [2008] and good agreement was found compared to using the uniform plane-wave method.

3.3 Network Calculation

Several methods have been developed for GIC calculation; two methods are described in this chapter namely: the system parameter (i.e., *a&b* parameter) method and the Nodal Admittance method. Both of these methods ignore the contribution of inductive components in the network because the variation of the electric field is assumed to be slow enough [Pirjola, 2002] and thus the entire transmission network can be modelled as a resistive network. The Nodal Admittance method is the method that was used in this dissertation.

System *(a&b)* parameter method

This method is based on the derivation by Lehtinen & Pirjola [1985] in which the system parameters, *a&b*, are calculated for each substation in the network. The "*a"* parameter is the value for the eastward surface potential of 1 V/km and the "*b"* parameter is the value for the northern surface potential of 1 V/km.

GIC flowing from the ground via the transformer neutral at every instant in time can be obtained by the following matrix:

$$I_e = \begin{pmatrix} I_{e1} \\ I_{e2} \\ I_{e3} \\ I_{e4} \\ I_{e5} \end{pmatrix} = \left(U + YZ\right)^{-1} J_e, \qquad (3)$$

Equation (3) is derived for a 5 node network. I_e represents the *a&b* network constants. The a*&b* network constants can be obtained by changing the elements of the column matrix J_e for an eastern and northern electric field of 1 V/km respectively. Where U is a 5x5 unit matrix and Z is a 5x5 diagonal matrix consisting of the earthing impedance which is made up of a sum of the resistances of the transformers with all three phases in parallel, and the actual or assumed earthing resistances. Y is the network admittance 5x5 matrix calculated from the line resistances of the network.

The Y matrix is defined by:

$$(i \neq j): Y_{n,ij} = -\frac{1}{R_{ij}^n}, (i = j): Y_{n,ij} = \sum_{k \neq i} \frac{1}{R_{ik}^n}, \quad (4)$$

The J_e is the 5x1 matrix defined by:

$$J_{e,i} = \sum_{j \neq i} J_{n,ji}, \quad (5)$$

$$J_{n,ji} = \frac{V_{ji}^0}{R_{ji}^n}, \quad (6)$$

$$V_{ji}^0 = \int_{s_{ji}} E_0 ds \quad (7)$$

Once the *a&b* parameters are calculated using equation (1-7) and after obtaining the electric field from equation (2), the GIC flowing in the each node is calculated as follow:

$$GIC(t) = aE_x(t) + bE_y(t) \quad (8)$$

This approach can only be applied using uniform electric field and uniform ground conductivity. Previous studies done on the Southern African network applied this method and found good correlation with the measured results [Koen, 2002; Koen & Gaunt, 2002].

Nodal Admittance Matrix method

This method is the described by Foss & Boteler [2006] and summarised by Trichtchenko et al. [2006]. **Figure 3-1** shows a representation of how GICs flow in the network.

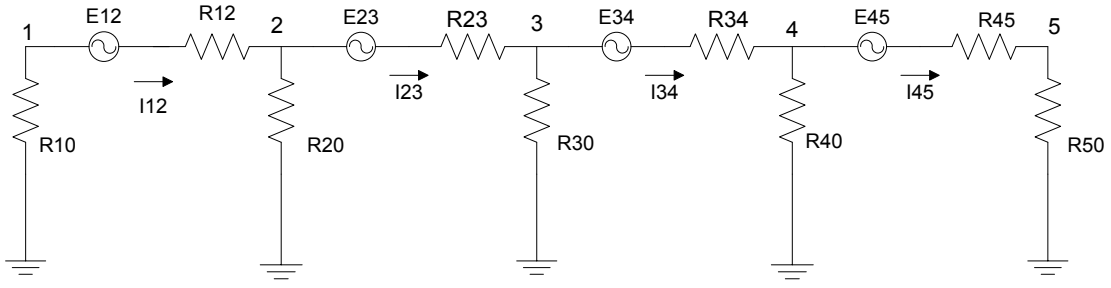

Figure 3-1: Network diagram showing Resistances, Induced EMFs and flow of GICs [Trichtchenko et al., 2006]

The substations of the network in **Figure 3-1** are represented by numbers, the R_{ij}'s are the line resistances and the R_{i0}'s are the substation grounding resistances. The voltage sources induced as a result of the geo-electric field induced in the network are shown by E_i's.

The source voltages and the transmission line resistances in **Figure 3-1** are converted to the Norton equivalence circuit shown in **Figure 3-2**. In the Norton equivalent circuit, the source voltage is converted to a current source using $J = YE$. The source voltages are indicated parallel to the transmission line while, the transmission line is represented by an admittance using $Y = \frac{I}{V}$.

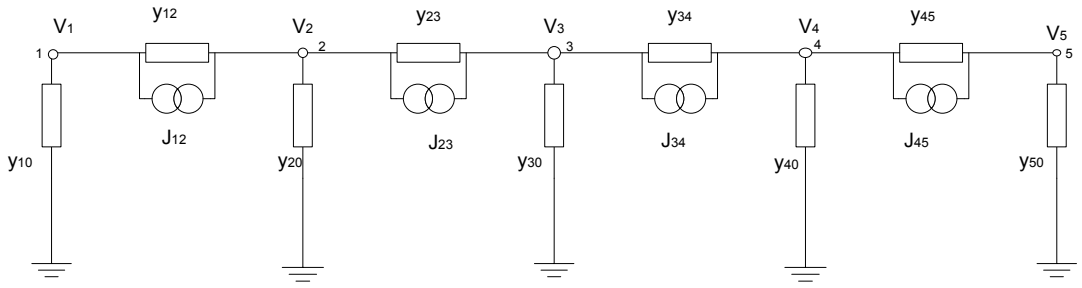

Figure 3-2: Network diagram showing admittance, current sources and nodal voltages [Trichtchenko et al., 2006]

From Kirchhoff's law, the sum of currents into a node is equal to the sum of currents coming out of a node. Applying this law, the following current equations are achieved:

$$-I_{12} = I_1 \tag{9}$$

$$I_{12} - I_{23} = I_2 \tag{10}$$

$$I_{23} - I_{34} = I_3 \tag{11}$$

$$I_{34} - I_{45} = I_4 \tag{12}$$

$$I_{45} = I_5 \tag{13}$$

The ground currents I_1, I_2, I_3, I_4 can be calculated using the source voltages where

$I_k = y_k V_k$ and $I_{k,k+1} = y_{k,k+1}(V_{k+1} - V_k)$ where k=1,2,3,4; V_K is the nodal voltages;

$$y_k = \frac{1}{R_k} \text{ and } y_{k,k+1} = \frac{1}{R_{k,k+1}}. \tag{14}$$

From Ohm's law, the current flowing in the transmission line between two nodes can be calculated from the potential difference between the two nodes and the current sources in parallel with the line. Using the above information and equations, the current equations can be re-written to the following equations [Trichtchenko et al., 2006]:

$$-J_{12-}-y_{12}(V_{1-}-V_2)=y_1V_{1-} \quad (15)$$

$$J_{12+}+y_{12}(V_{1-}-V_2)-J_{23}-y_{23}(V_2-V_3)=y_2V_2 \quad (16)$$

$$J_{23+}+y_{23}(V_{2-}-V_3)-J_{34}-y_{34}(V_3-V_4)=y_3V_3 \quad (17)$$

$$J_{34+}+y_{34}(V_{3-}-V_4)-J_{45}-y_{45}(V_4-V_5)=y_4V_5 \quad (18)$$

$$J_{45+}+y_{45}(V_{4-}-V_5)=y_5V_5 \quad (19)$$

Equation (15)-(19) can be manipulated and re-arranged into a matrix form and this leads to a system with 'n' equations and 'n' unknown as seen below:

$$\begin{bmatrix} J_1 \\ J_2 \\ J_3 \\ J_4 \\ J_5 \end{bmatrix} = \left[\begin{array}{ccccc|c} y_1+y_{12} & -y_{12} & 0 & 0 & 0 & V_1 \\ -y_{12} & y_{12}+y_2+y_{23} & -y_{23} & 0 & 0 & V_2 \\ 0 & -y_{23} & y_{23}+y_3+y_{34} & -y_{34} & 0 & V_3 \\ 0 & 0 & -y_{34} & y_{34}+y_4+y_{45} & -y_{45} & V_4 \\ 0 & 0 & 0 & -y_{45} & y_4+y_{45} & V_5 \end{array}\right] \quad (20)$$

The current sources J_k's can be obtained as follows:

$$J_1=-J_{12};\ J_2=J_{12}-J_{23}$$
$$J_3=J_{23}-J_{34};\ J_4=J_{34}-J_{45}$$
$$J_5=J_{45} \quad (21)$$

The Voltages V_k's can now be obtained by matrix inversion using equation (20). Multiplying the Voltages obtained with the neutral admittance, the currents flowing in the ground to/from the substation can be obtained.

One of the benefits of using the Nodal Admittance method is that the method has the capability of accepting non-uniform electric field data for each region in the network.

3.4 GIC Monitoring and Measurements

Real time magnetometer readings in the Southern African region are done by SANSA at different magnetic observatories located in Namibia at Tsumeb and Keetmanshoop and in South Africa at Hermanus and Hartebeesthoek.

Using the relationship between the E-field, the ground conductivity and the magnetic field measured, the electric field across the network can be obtained. Previously, it was assumed that there is uniform ground conductivity for the entire network and this resulted in the same electric field across the entire network. However, from recent studies, using a non-uniform ground conductivity and non-uniform electric field was found to reduce the differences between the measured and calculated GIC results [Bernhardi et al., 2008].

From literature, two methods exist for GIC measurements. One method is to install two magnetometers, one under the line and another further away, to measure the magnetic field induced as a result of the GIC flowing in the lines. The other method is to install Hall-effect transducers in the transformer neutral to measure GIC directly. Applying appropriate filtering to the measured data, a DC current flowing in the transformer neutral [Lianguang et al., 2005].The second approach also includes installation of CTs and VTs on transformer phases. All these measurements are fed to a data logger and can be accessed locally or remotely.

3.5 Chapter summary

Derivations of the electric field using different modelling techniques were covered. GIC calculation techniques namely using the *a&b* parameter method and the Nodal Admittance method were described in detail. The Nodal Admittance method was chosen for this dissertation because it offers flexibility since it can accept both uniform and non-uniform electric field data. Finally, two GIC measurement techniques were discussed namely directly measuring GICs in the transformer neutral or indirectly by measuring magnetic field induced under the transmission line. The direct method is preferred for this dissertation.

Chapter 4

Test network

After discussing the differences between the a&b parameter method and the Nodal Admittance method for GIC calculations, it is important to first validate the Nodal Admittance method before it is applied for GIC calculations as proposed for this dissertation. In this chapter, the Nodal Admittance method is validated using previously published data calculated using the a&b parameter method. The validation process was done on the 2002 Namibian network as used in a previous study and under the same conditions. This was performed as a first stage of the validation process for the Nodal Admittance method to check whether the results obtained using the two methods agree before adopting the Nodal Admittance method for calculations and validate it further using measured results.

4.1 Model data inputs

Previously, the a*&b* parameter method was used by Koen [2002] to calculate GICs on the 2002 Namibian transmission network. Good correlations was found between the results obtained using the *a&b* parameter method and the measured results.

Having discussed the differences between the *a&b* parameter method and the Nodal Admittance method for GIC calculation in the previous chapter, it is useful to investigate how closely the results of the two methods compare under similar conditions.

In this section, the MATLAB program developed by Oyedokun et al. [2013], based on the Nodal Admittance method, will be used to calculate GICs on the 2002 Namibian network under the same conditions as the study done by Koen [2002]. The results will be compared to those obtained by Koen [2002] using the *a&b* parameter method. This will serve as a first validation test for the new improved version of the Nodal admittance method.

The input parameters used by the Nodal Admittance method are:

- Line resistances
- Substation neutral resistances
- Substation positions and connections
- Geomagnetic field data

The transmission line parameters were obtained from NamPower network operators while geomagnetic data are obtained from the South African National Space Agency (SANSA) from the different magnetic observatories. The Electric field data were given in units of V/km. It is important to note that, the inductive components of the network were neglected in the model because GICs have a frequency ranging from 0.1 mHz -10 mHz. This means that the inductive components of the network are relatively small in magnitude compared to the resistive components of the transmission lines at this frequency and for this reason it can be ignored.

From Chapter 3 it was shown how the transmission network can be represented to derive how GICs are calculated in the network using the Nodal Admittance method. GICs enter the transmission network via transformer neutral conductors which then split equally amongst the three phases of the transformers and thereafter to the rest of the network through the transmission lines. This approximation is only valid in the case where there are no autotransformers in which case GICs might flow via series winding to the next transformer and not necessarily terminate at the local earthing point. In this dissertation, the presence of autotransformers was neglected to simplify the calculation.

4.2 MATLAB Program description

The MATLAB program on the Nodal Admittance method was developed by Oyedokun et al. [2013]. At the beginning of the program, files containing line parameters, substation coordinates and electric field data are loaded. The files should be saved with a *.txt* extension. Thereafter, the electric field component induced on each line is calculated while putting the orientation of the line in consideration.

After the electric field components induced on each line are calculated, the corresponding voltage sources are obtained by multiplying the electric field data (V/km) with the corresponding line lengths (km). Thereafter, the voltage sources are used to calculate the Norton equivalent current sources for each transmission line. The line resistances are used together with the current sources to calculate the currents flowing in each transformer's ground neutral conductor.

The program was tested using two simple circuits to model the GIC flowing at each substation when the electric field is aligned at 45, 90, and 180 degrees. The electric field data was chosen specifically to be aligned at those degrees to test how the field alignment affects GIC flow. The parameters used are as follows: **Table 4-1 for** Circuit 1 (East-West Line) and **Table 4-2** for Circuit 2 (North-South line). The circuit diagrams are shown in **Figure 4-1** and **Figure 4-2**.

Table 4-1: Network parameters for circuit 1

	Nodal Admittance	Substation coordinates	Line Admittance	Line Lengths
Substation A	1	(30, 50)		
Substation B	1	(50, 50)		
Line A-Line B			1	100

Figure 4-1: Circuit 1 diagram

Table 4-2: Network diagram for circuit 2

	Nodal Admittance	Substation coordinates	Line Admittance	Line Lengths
Substation C	1	(30, 50)		
Substation D	1	(30, 40)		
Line C-Line D			1	100

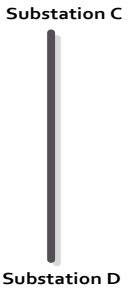

Figure 4-2: Diagram for circuit 2

The GIC flowing at each substation under different electric fields with same magnitude at different angles were obtained using the parameters given in **Table 4-1** and **Table 4-2** as follows:

Table 4-3: GIC (A) results for circuit 1 at different electric field alignments

	GIC[A] E-field at 45 degrees (-0.03, -0.03)	**GIC[A]** E-field at 90 degrees (0, -0.042426)	**GIC[A]** E-field at 180 degrees (-0.042426, 0)
Substation A	1	0	1.4142
Substation B	-1	0	-1.4142

Table 4-4: GIC (A) results for circuit 2 at different electric field alignments

	GIC[A] E-field at 45 degrees (-0.03, -0.03)	**GIC[A]** E-field at 90 degrees (0, -0.042426)	**GIC[A]** E-field at 180 degrees (-0.042426, 0)
Substation C	-1	-1.4142	0
Substation D	1	1.4142	0

Applying the Nodal Admittance method to simple circuits show consistency with electromagnetic theory. The maximum GIC magnitudes were experienced when the electric field was at 180 degrees in the East-Western line while that of the North-Southern line was experienced when the electric field was at 90 degrees. In both cases the maximum GIC magnitude was experienced when the electric field is parallel to the line.

4.3 Study system

As previously mentioned, the first validation process includes the use of Nodal Admittance method to calculate GICs on the 2002 Namibian transmission network under the same conditions as the study previously done by Koen [2002] using the *a&b* parameter method.

In this dissertation, it is important to note that the modelling process assumes constant network parameters for the entire duration of the study. **Figure 4-1** shows the case study used in this dissertation to validate the Nodal Admittance method. The case study used is the 2002 Namibian transmission network obtained from Koen [2002]. The 2002 transmission network composed of 10 substations. The Namibian network is connected to the South African network via Aries substation. In this study, only transmission lines of 400 kV and 220 kV spanning over 100 km in length were considered. The earthing resistance was assumed to be 0.8 Ω for all the substations in the calculation technique for this dissertation.

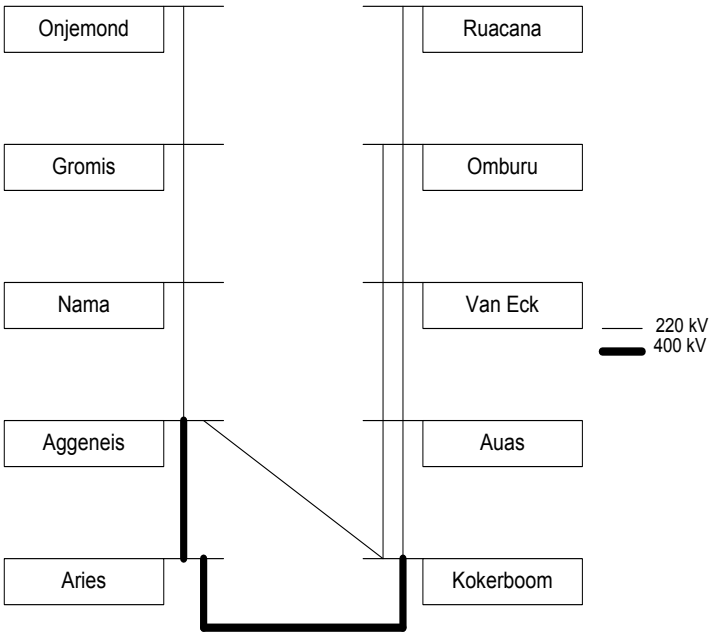

Figure 4-3: Case study system: The Namibian 2002 transmission network [Koen, 2002]

Table 4-1 and **Table 4-2** shows the parameters for the 2002 transmission network [Koen ,2002].

Table 4-5: Network parameters of the 2002 Namibian transmission lines

Line Description	Admittance	Length [km]
Oranjemond/Gromis	0.336	130
Gromis/Nama	0.575	76
Nama/Aggeneis	0.442	99
Aggeneis/Aries	0.662	196
Aggeneis/Kokerboom	0.087	337
Aries/Kokerboom	0.362	420
Kokerboom/Auas	0.341	446
Kokerboom/Auas	0.064	460
Auas/Van Eck	1.010	29
Auas/Van Eck	1.087	29
Van Eck/Omburu	0.192	163
Van Eck/Omburu	0.190	165
Omburu/Ruacana	0.155	524

Table 4-6: Substation parameters of the 2002 Namibian transmission network

Substation name	Latitude [deg]	Longitude [deg]
Aggeneis	-29.3	18.8
Aries	-29.49	20.79
Gromis	-29.6	17.18
Kokerboom	-26.54	18.12
Nama	-29.63	17.88
Oranjemond	-28.54	16.6
Ruacana	-17.4	14.22
Omburu	-21.5	16.03
Auas	-22.59	17.37
Van Eck	22.52	17.08

The electric field data used in this study corresponds to the 3 hour period of 21:00 to 24:00 on the 13th March 1989 magnetic storm obtained from the Hermanus Magnetic Observatory using the plane wave method and the uniform ground conductivity of σ=1 mS/m, taking M=10 where M is the number of previous magnetic field data used to calculate the present electric field samples value. This study was done to validate the Nodal Admittance method using published data which were obtained using the *a&b* parameter method. This validation process was first done in a previous study by Simon et al. [2013] using the 2002 Namibian transmission network under the same conditions as the initial study by Koen [2002].

Table 4-3 shows the network constants calculated for the 2002 Namibian transmission network [Koen, 2002].

Table 4-7: *a&b* parameters used for GIC calculations on the 2002 Namibian transmission network [Koen, 2002]

Substation	a-Value	b-Value
Oranjemond	26	-19
Gromis	-23	-17
Nama	-21	-7
Aggeneis	-25	-14
Aries	-85	116
Kokerboom	-25	-24
Auas	54	-6
Van Eck	33	12
Omburu	3	-16
Ruacana	63	-26

The results shown in **Figure 4-2** and **Figure 4-3** shows a comparison between results obtained using the *a&b* parameter method and the Nodal Admittance method.

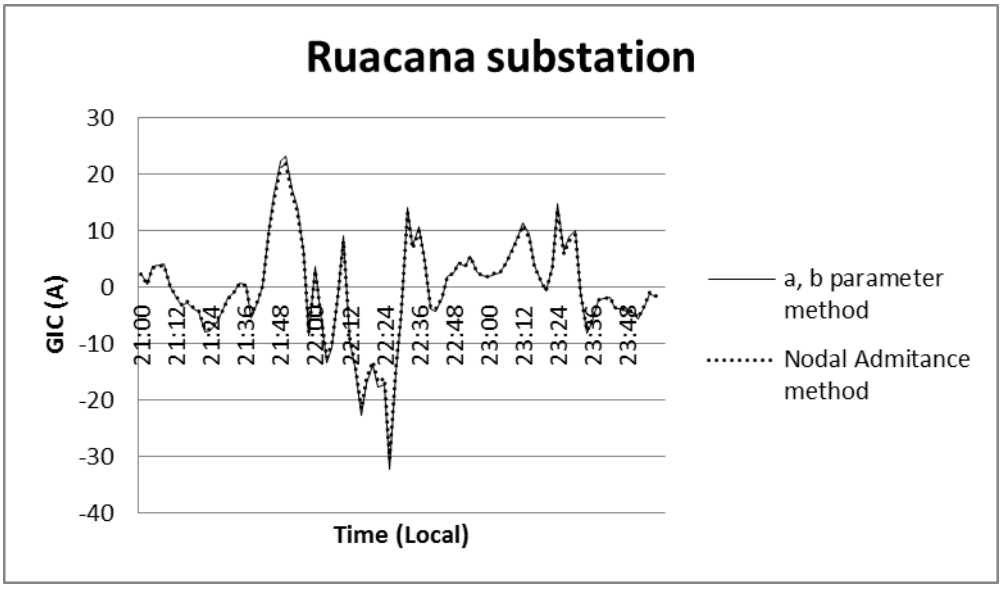

Figure 4-4: Simulated results for Ruacana substation using *a&b* parameter and Nodal Admittance method

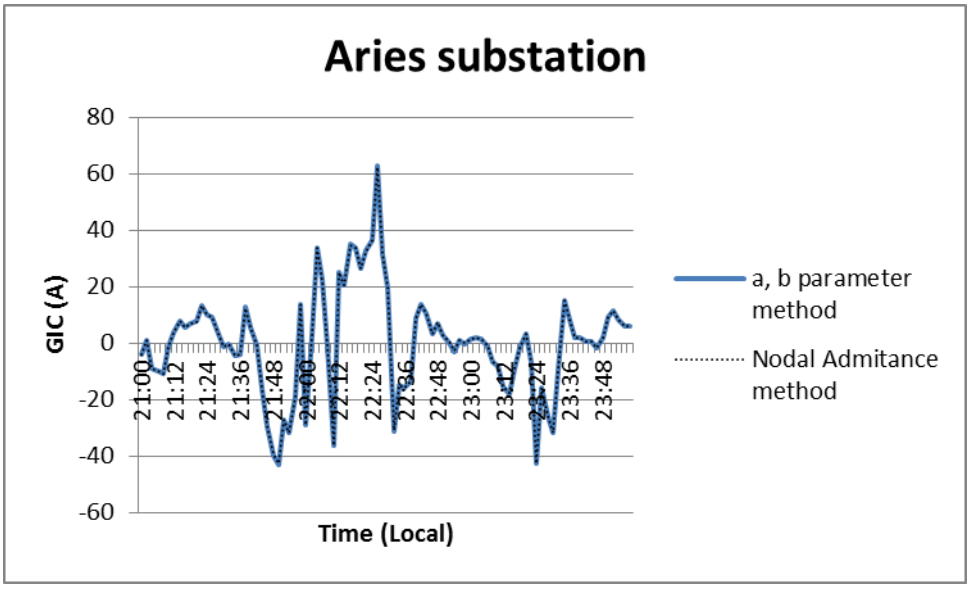

Figure 4-5: Simulated results for Aries substation using *a&b* parameter and Nodal Admittance method

Table 4-3 shows GIC exposure of all the substations in the 2002 Namibian transmission network using the March 1989 geomagnetic data recorded in Hermanus. This will aid the choice of substations for GIC measurements.

Table 4-8: Absolute GIC maximum values for the 2002 using the Nodal Admittance method

Substation name	GIC max [A]
Aggeneis	7
Aries	63
Gromis	7
Kokerboom	9
Nama	6
Oranjemond	15
Ruacana	33
Omburu	5
Auas	22
Van Eck	7

4.4 Discussions

The main purpose for this chapter was to validate the Nodal Admittance method using previously published data obtained using the *a&b* parameter method. This was done by comparing the results obtained using the Nodal Admittance method with those previously published by Koen [2002] for the Namibian network using the *a&b* network parameter method under the same conditions. From **Figure 4-2** to **Figure 4-3**, the results obtained using the two methods show good correlation. This is good enough for the first validation step. Further qualification of the model is obtained by comparing the modelled results of the existing Namibian transmission network with the measured GIC data and this will be done in the next chapters.

The exposure of the 2002 Namibian transmission network is also shown in **Table 4-3**. Aries substation was found to have the maximum absolute GIC magnitude. Since Aries substation is part of the South African network, it follows that the substations with highest GIC magnitude in the 2002 Namibian transmission network were Ruacana followed by Auas and Oranjemond. The rest of the substations showed GIC magnitudes of less than 10 A.

4.5 Chapter summary

The Nodal Admittance method as proposed for this study has been tested under the first validation stage using previous published GIC data. The Nodal Admittance model offers ease of use for GIC calculations, as it offers flexibility to use both uniform and non-uniform electric field data and network parameters are easily modifiable. The exposure of the Namibian substations to GICs was performed and Ruacana substation was found to have the highest GIC magnitude in the network followed by Auas and Oranjemond substation. The next validation process is to compare calculated results with measured results which will be done in the following chapters.

Chapter 5

GIC Measurement and Monitoring

The modelled results are not enough to conclude on the magnitude of GICs flowing in the network. Thus, measurements should be taken in order to verify modelled results.

This chapter discusses the equipment installed for GIC measurements on the Namibian transmission network. The criteria used to select the equipment used for the study are also discussed in this chapter. The complete equipment set-up was first tested in the lab on a published laboratory set-up. Thereafter, the substations chosen for measurements are stated and the motivations for choosing them are discussed.

5.1 Objectives of monitoring devices

The objective of GIC monitoring devices is to enable the utility to record data and collect sufficient data for analysis and draw correlations with predicted GIC results. This will later allow an investigation on transformer's response to GICs. Monitoring systems makes it possible to easily apply future extensions such as alerting system operators when high GIC values are recorded. This will enable the utility to make informed decisions in terms of switching some lines off to avoid the possibility of high equipment damage.

5.2 Characteristic of monitoring devices

GIC flows into the network via transformer neutrals. Thereafter, it divides into equal magnitudes among the three phases of the transformer. GIC presence in the transformer may lead to half-cycle saturation which may result in increased absorption of non-active power, increased of noise levels, transformer's over-heating, and generation of harmonics. For the purpose of this dissertation, only phase currents and voltages as well as the neutral currents will be monitored.

The characteristic of measuring devices are:

- *Measure the neutral current flowing in the neutral conductors of the transformers*
  Under transformer's balanced operating conditions with no GICs, the current flowing in the transformer neutral is zero. However, in the presence of GICs the current in the transformer neutral is a "quasi" DC current also referred to as GIC. Thus any current device connected to the neutral conductor of the transformer will measure GICs.
- *Measure phase voltages and currents in the 3-phases of the transformer*
  The three phase voltages and currents can be used to calculate active and non-active power. From literature, an increase in non-active power indicates the presence of GICs as well as a reduced power factor. Voltages and currents in the transformer phases will be measured.
- *Measure harmonic content in the voltage and currents waveforms*
  The three phase voltages and currents recorded will be used to calculate harmonic contents in the data. Harmonic analysis will also be used to show if any harmonic signatures are observed in the data under specific network conditions.
- *Record all data using a data logger*
  The data logger will be used to record and store the measured three phase voltages and currents and the neutral current for easy access and further offline analysis.
- *Record Measurements in real-time*
  Real-time data allows the utility to take quick decisions if necessary to reduce network equipment damage in the presence of high GIC flow.

5.3 Equipment selection

One of the research questions to test the hypothesis was to determine how GIC measurements will be done in the Namibian network. In this section, the selection process of different measurement devices to be used in this dissertation is discussed.

Under normal conditions, the transformer neutral conductor carries no 50/60 Hz current because the sum of the AC currents in the three phases is zero. In the presence of GICs, a “quasi” DC current is induced in the transformer neutral conductor. Measuring GICs directly in the neutral conductor gives information about the currents flowing through transformer windings.

Measurements of GICs can be done by positioning a clamp on Hall-effect sensor around the transformer neutral conductor to pick up all the currents flowing in the neutral conductor. Furthermore, GIC monitoring also involves measuring transformer AC phase currents and voltages.

To be able to take phase current measurements, there is a concern that some of the Current Transformers (CTs) used in the substations might not be connected in the way which is suitable for GIC study. There are two ways in which the CTs can be connected, one such approach is to connect the CTs between each phase and neutral and the second approach is to connect CTs between each two neighbouring phases. The second approach is not favourable for GIC study because for GIC study, all the three phase current measurements are necessary to perform calculations such as power factor, non-active power according to Gaunt & Malengret [2012].

For the purpose of GIC study, in the case that the CTs at the chosen sites are connected between two neighbouring phases, the circuit to be used for measurements will need to be altered to give meaningful results. Since the only thing missing in this approach is the neutral, there will be a need to install new CTs and/or Voltage Transformers (VTs) and create a new reference.

It was later discovered that CTs and VTs in all the substations in the network were connected between each phase and neutral of the transformers which is favourable for this study and thus no circuit alterations were necessary.

Another concern was that there might not be unused cores at some of the substations in the network and this could be a problem especially with regards to CTs. One needs to be extremely careful when open circuiting CTs because when a CT is open circuited, it acts like a VT with a large voltage across it which can lead to power outages/disruption and can also

cause threat to lives. In such a case, clamp-on CTs will be preferable to avoid disrupting existing measurement systems.

5.4 Equipment selection criteria

In choosing equipment for GIC monitoring, there are specific requirements that should be considered to ensure that the final choice of equipment will ultimately provide reliable measurements. From literature, GIC enter the transmission network through the transformer neutral conductor, thereafter it divides equally between the three phases to the entire network. Therefore, the measuring devices to be used will work under this assumption and only monitor GICs in the transformer neutral conductor and also measure the three phase voltages and currents. Only the Low Voltage (LV) side of the transformer will be considered for voltage and current measurements.

Below are the criteria used in choosing the appropriate equipment for GIC measurements:

- Sampling frequency range.

  The sampling frequency was chosen to measure up to the 10^{th} harmonic in order to be able to analyse any possible harmonic signatures observed in the measurements. To be able to measure up to the 10^{th} harmonic which corresponds to a frequency of 500 Hz, the sampling frequency should be greater than 1000 Hz to meet the Nyquist criterion. The Nyquist sampling theorem states that the minimum sampling rate to accurately reconstruct a waveform should be twice the highest frequency needed for the waveform.

- Continuous sampling

  The data logger to be chosen for the study should be able to perform continuous sampling and provide sufficient storage to be able to process data offline depending on the need for the research.

- Data storage
  The measurements are planned to be taken for a period of 2 months or longer depending on the need for the research and when a CME occurs.
- Take Bipolar measurements
  Since waveforms to be measured could be both positive and negative, the equipment to be used should be able to take bipolar measurements.

- Current measuring equipment
  The current measuring equipment should be able to take both AC and DC current measurements and should be able to handle the expected maximum GICs based on previous data available.
- Equipment connection to the network
  Equipment to be used for GIC measurements should not cause any disruption to existing measurement systems.

Based on the above requirements, measuring equipment were chosen and brief details for the equipment chosen are discussed in the following sections:

5.5 Data logging system

A correlation between actual GIC measurements and simulated results has been established in the literature using different algorithms [Bernhardi, 2008; Koen, 2002]. A data logger will be utilized to record measurements which will then be used to compare measured results with modelled results with an aim to validate the calculation technique.

For continuous measurements, the data logger system used in this dissertation consists of voltage and current modules to record both phase voltages and currents respectively. The logging system used is a National Instrument (NI) product and it has gained international usage in simulation, data acquisition, simulation, data processing, instrument and control [Wells & Jeffery, 1996]. NI products make use of LABVIEW programming language short for **Lab**oratory **V**irtual **I**nstrumentation **E**ngineering **W**orkbench. A front view of the NI cDAQ (data acquisition) and the modules used in this dissertation is shown in **Figure 5-1** and **Figure 5-2** respectively.

Figure 5-1: NI cDAQ-9184, Compact DAQ chassis

Figure 5-2: Voltage module (NI 9205) and Current module (NI 9225)

The voltage module accepts voltage inputs within a ±10 V range and it has 37 channels. For these reasons, voltage transformers (VTs) were used to step down the voltage before connecting to the voltage module to ensure that the voltage is within the acceptable range. The current module has three input channels and it will be used for logging two phase currents and one neutral current.

5.6 Hall-effect transducers

To avoid disruption of existing current transformers (CTs), Hall-effect transducers were used for current phase measurements and for neutral current measurements. The Hall-effect transducers chosen had a capability to measure both AC and DC.

Hall-effect transducers transform a magnetic field signal, induced by any current carrying wire, into a voltage. For this reason, to avoid interference from other conductors, the transducer should not be placed in close proximity to any other conductor to ensure that the only current being picked up is the correct current. In addition, the transducer should be rated high enough in order to pick up maximum neutral currents previously predicted for the Namibian network from previous geomagnetic storms.

Each transformer neutral conductor has a different diameter and thus different Hall-effect transducers were considered to compensate for the varying diameters. Care must be taken when using the transducers to ensure that they are not in close proximity to nearby conductors in order to prevent measurements of unwanted signals. Furthermore, they should be mounted properly to ensure that they are detecting all the currents flowing in the conductors.

Figure 5-3 below shows the different current probes that were used in this dissertation:

Figure 5-3: Current probes used in this study: Prosys Probe CP30 & Universal Probe H20.3C

The specifications for the Hall-effect transducers are shown in **Table 5-1**.

Table 5-1: Specifications for the Hall-effect transducers

MODEL	CP 30	H20.3C
Current range	5 mA to 30 A or AC peak	2000 A/ 200 A
Output sensitivity	100 mV/A	1 mV/A or 10 mV/A
Frequency range	DC to 20 kHz	DC to 1 kHz
Jaw capacity	25 mm Ø	72 mm Ø

The CP30 Hall-effect transducers were used to measure phase currents while the H20.3C Hall-effect transducers were used to measure neutral currents. The CP30 Hall-effect transducers were connected to the Low Voltage (LV) side of the CTs. CTs are designed to take AC measurements and thus the measurements using the Hall-effect transducers might not detect all the DC currents flowing in the three phases. Furthermore, the saturation of CTs might also affect the Hall-effect transducer's measurements. Putting the above restrictions in consideration, the CP30 Hall-effect transducers were used in this dissertation.

A complete installation of a single logging system unit for one transformer comprises of the following:

- One NI cDAQ (data logger)
- 1 voltage module
- 1 current module
- 3 Hall-effect transducers
- 1 AC-DC converter (9 V Mean Well AC-DC NES-100 converter)
- Voltage transformers (VTs)

The measurements are fed to the data logger via an Ethernet cable using a sampling frequency of 1.613 kHz and the data is stored on a local workstation computer.

5.7 Laboratory test

After choosing the equipment to be used for GIC measurements, they were first tested using a laboratory set-up developed by Chisepo et al. [2013] before installation on the Namibian transmission network. The laboratory set-up involved a bank of three-limb single phase source transformers and a load transformer. The set-up used the Yokogawa WT1600 Digital Power Meter to take instantaneous voltage and current waveforms. The source transformers supply a load composed of a balanced bank of power resistors in each phase. A three phase variac was used as voltage source supplying the transformers. **Figure 5-4** below shows a single phase diagram of the laboratory set up arrangement.

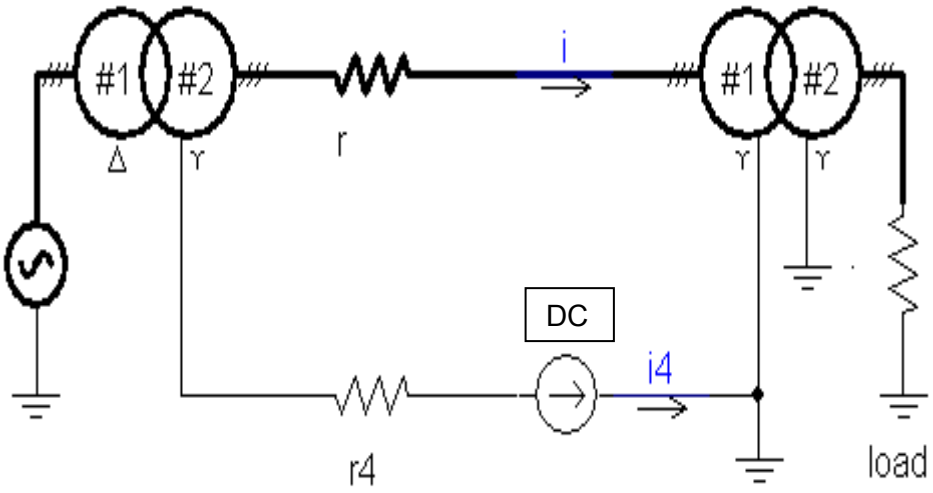

Figure 5-4: Single phase diagram of the laboratory arrangement [Chisepo, 2013]

Figure 5-5 shows the basic equipment connection used for GIC measurements in this dissertation. The voltage and current measurements are taken on the LV side of the 3-phase transformer as shown. The outputs of the Hall-effect transducers (CP 30's and H20.3C) are directly connected to the data logger. The Hall-effect transducers give out a voltage output and this is converted to a current output using the ratio for the Hall-effect output sensitivity as indicated in the specifications in **Table 5-1**.

The voltage transformers (VTs) are also connected directly to the data logger. One important aspect to consider is to ensure that the inputs from the VTs are in the input range acceptable by the data logger according to the specifications.

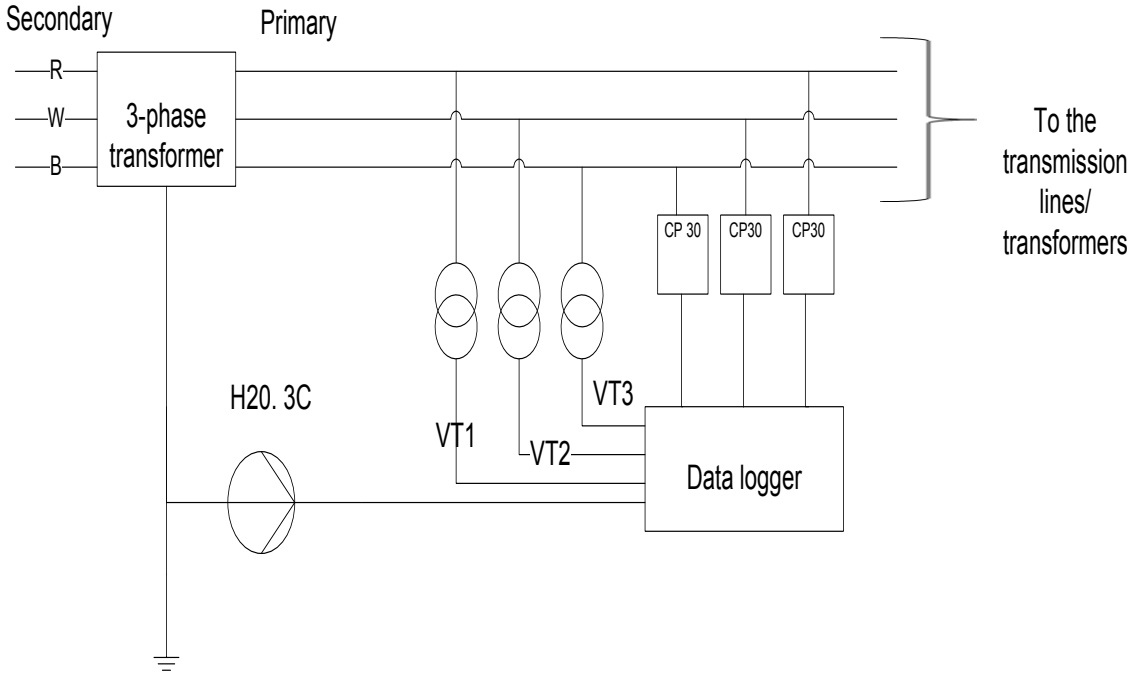

Figure 5-5: Basic equipment schematic

Preliminary tests were done on individual equipment before connecting to the set up as follows. All the VT's were tested to confirm the transformer ratios and the correct ratios were used to calculate the phase voltages flowing in the three phases. The Hall-effect transducers were tested by clamping them onto the transformer neutral conductor with a known DC current flowing to confirm that the Hall-effect transducers were measuring the correct currents.

To test the equipment set up, a DC voltage was injected in the transformer neutral using a 1.5 V D battery and using a voltage divider to vary the DC voltage injected at any particular instance see **Figure 5-4**. The Yokogawa Power Meter was used to measure the DC

components in the transmission lines while the LEM module was used to measure the exact DC injected in the transformer neutral from a D battery. The Yokogawa Power Meter readings were compared to those recorded by the data logger using the proposed equipment shown in **Figure 5-5**.

There were two test scenarios implemented to test the equipment set up namely: full load with no GIC injected and full load with a known GIC injected in the transformer neutral. The measured results using the proposed equipment set up were compared with the Yokogawa Power Meter readings and were found to agree.

LABVIEW, the programming language used in this dissertation for data logging, is composed of user interfaces making it easy to use. LABVIEW consists of two components namely the front panel and the block diagram. The front panel component consists of all the controls and indicators used to control and view the signals being measured in real time while the block diagram component contains Virtual Instruments (VIs) used in the program to show the program flow. The block diagram and front panel used in this dissertation are shown below in **Figure 5-6** and **Figure 5-7** respectively.

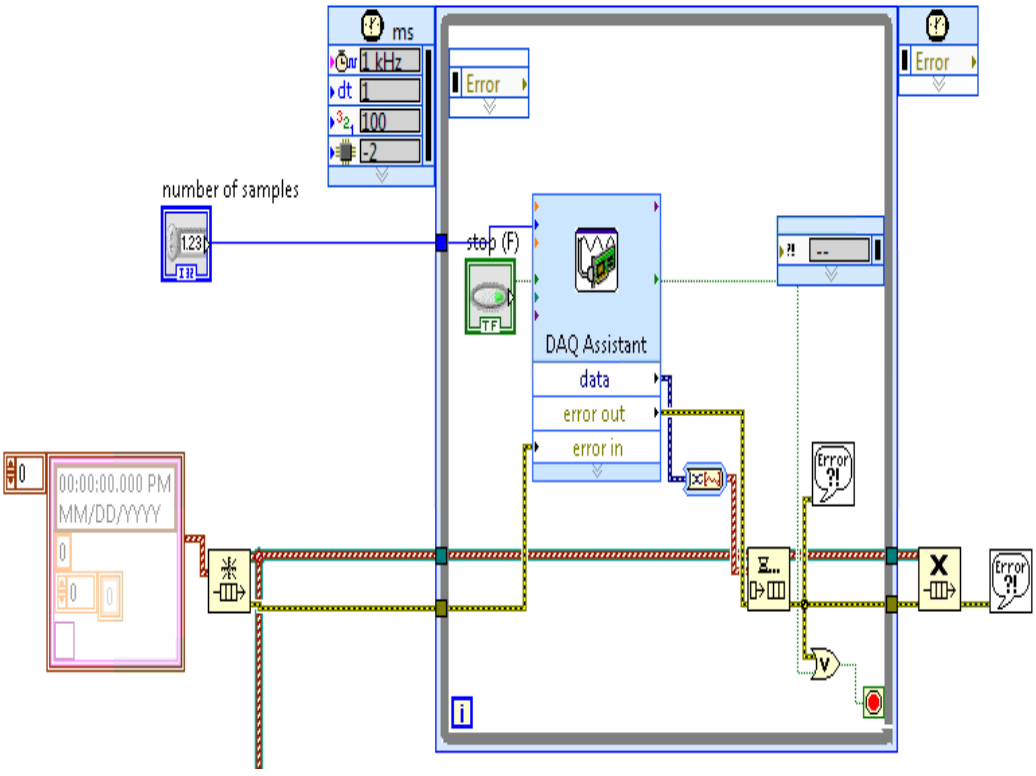

Figure 5-6: Block diagram used in Labview for taking measurements

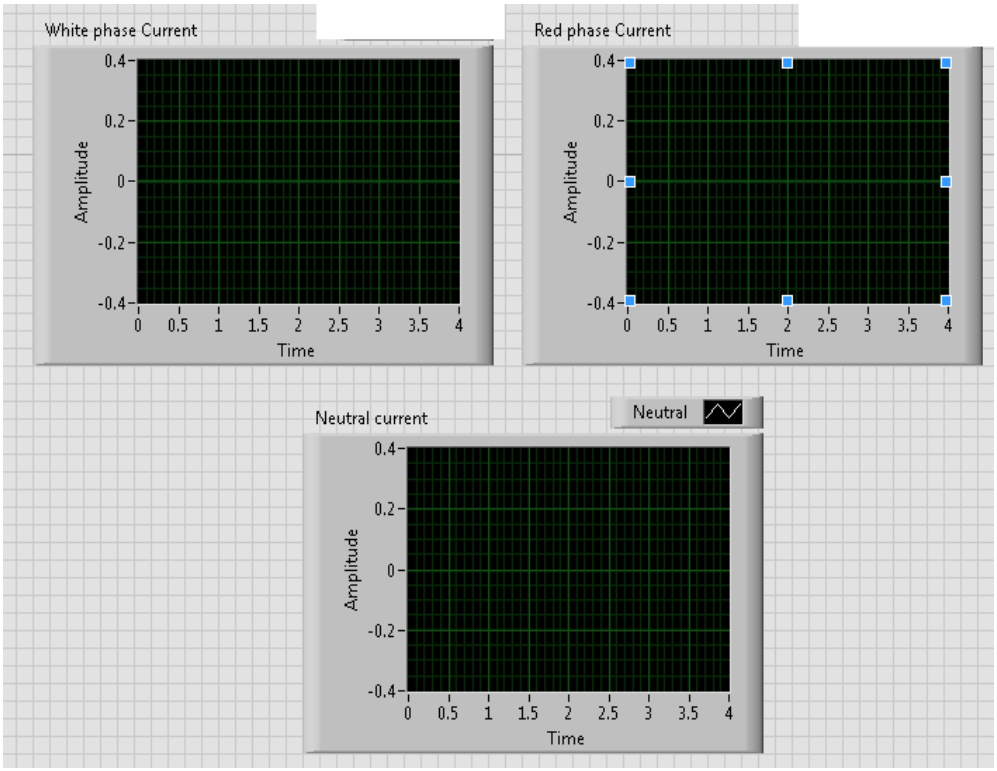

Figure 5-7: Front panel in Labview showing the two phase currents and the neutral current being measured

5.8 The Namibian transmission network

The Namibian transmission network consists of long transmission lines. The Ruacana substation is approximately 1160 km west of the Zambezi substation and 1600 km north of Aries; the Ruacana-Omburu 330 kV line is 521 km long and the Kokerboom-Auas line is 446 km long both being single line sections. **Figure 5-8** shows the map of the NamPower transmission network as of 2012 which will be used in this dissertation. The network has 21 nodes and a HVDC response circuit. Transmission line voltages range from 400 kV to 66 kV.

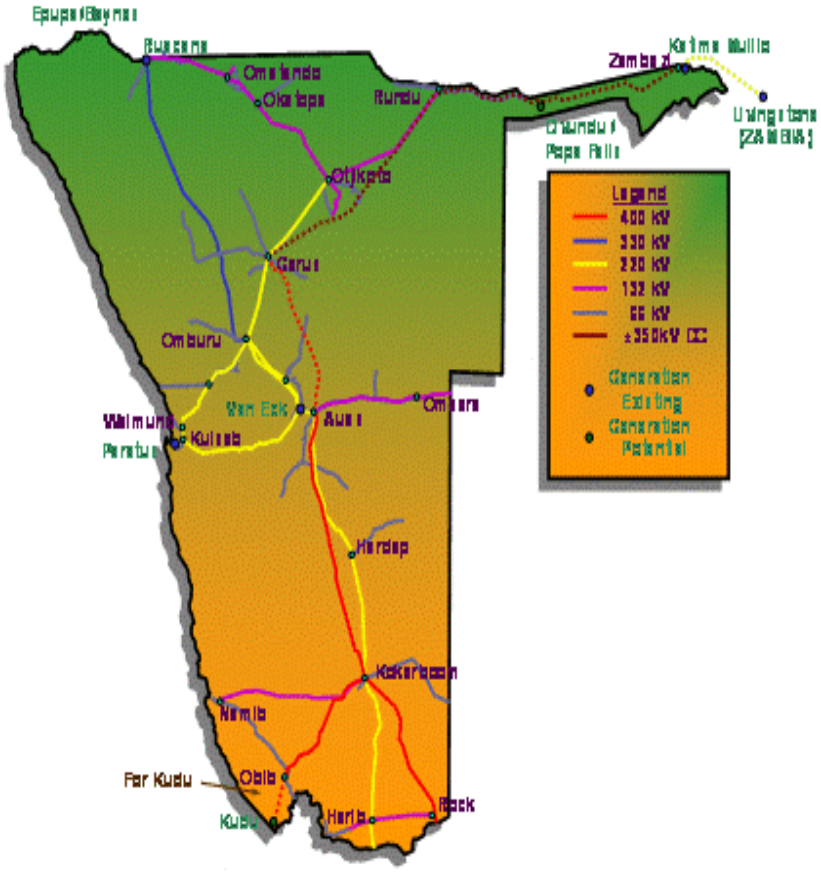

Figure 5-8: The Namibian transmission network [www.nampower.com.na]

One of the research questions stated in chapter one was to investigate what measurement techniques are suitable for the Namibian transmission network and this entails choosing substations where the measurements will be made. In choosing the measurement sites, it was necessary to investigate which substations are more susceptible to GICs in the network to consider them for monitoring. This was done by a simulated exposure of the 2012 Namibian network to one of the previous strong solar storms.

The Nodal Admittance method was used to calculate GICs on the current network using uniform electric field of the 13th March 1989 geomagnetic storm. The network parameters of the current Namibian network are shown in the appendix, however the substation coordinates where omitted from the appendix because they are NamPower confidential data.

Table 5-2 shows GIC maximum magnitudes for each substation in the current Namibian transmission network.

Table 5-2: GIC magnitude for the current Namibian transmission network using the electric field from the 13th March 1989 storm

2012 Namibian transmission substations	Absolute Max GIC [A]
Aggeneis	9
Aries	60
Kokerboom	20
Ruacana	30
Omburu	7
Auas	11
Van Eck	4
Khan	5
Trekkopje	5
Rossing	1
Walmund	3
Kuiseb	5
Gerus	6
Otjikoto	5
Osona	1

Hardap	2
Obib	13
Karas	1
Harib	3
Oranjemond	12

Aries substation was found to have the highest GIC magnitude but since it is part of the South African network, it was not considered for GIC measurements. Nonetheless for the substations in the Namibian transmission network, maximum GIC magnitudes where observed for Aries substation followed by Ruacana, Kokerboom and Obib substation. Kokerboom substation was not considered for measurements because it is connected to many nodes at different voltage levels which may introduce more complications on the installations of measurement devices and calculation techniques to be adopted. On the other hand, Obib substation was considered because it is connected to one node which is preferable to simplify calculations and comparisons between modelled and measured results as well as the installation procedure.

Subsequently, the Ruacana and Obib substation were chosen for GIC measurements based on past simulated results obtained using past geomagnetic storms, substation connectivity, substation location and historical events. Further motivation for choosing the two sites and more details about these sites are given in the next sections.

5.9 Ruacana substation installation

The Ruacana power substation is situated in the Northern part of Namibia. It is a hydro power station with four generation 11 kV-330 kV transformers. One of the reasons for motivating Ruacana substation is because, previously it was reported that in 2003, a two-year old generation transformer was damaged during a solar maximum of that cycle and the damage is reported to have been caused by GICs [Zatjirua, 2005]. To date, no GIC measurements were taken on the Namibian transmission network and thus the GIC magnitude which could have caused damage to the two-year old transformer is not known. Hence, it will be of benefit to NamPower to measure what maximum GIC magnitudes are flowing at the substation during a geomagnetic storm day to give an indication of the correlations between GIC magnitudes and possible equipment damage.

Apart from the above reasons, Ruacana substations was also chosen because since it is a power station whose there are always personnel on site, and if there is any problem with the installations there are NamPower personnel available to assist.

GIC measurements were done on two generation transformers namely on generation transformer 1 and generation transformer 3. One reason for choosing generation transformer 1 is because there is a Dissolved Gas Analysis (DGA) online monitor installed on it and measurements are taken on daily basis. This could add an important aspect to the research in the cases when the transformer is discovered to have failed and the dissolved gases in the transformers will be analysed to compare them to the time of a possible geomagnetic storm that took place closer to that time. The Ruacana single line diagram is shown in the Appendix.

5.10 Obib substation installation

The Obib substation is located in the Southern part of Namibia. It consists of two 400 kV–66 kV transmission transformers. The Obib substation is fed by a 400 kV transmission line from Kokerboom substation and is only feeding the Scorpion Zinc mine through a 66 kV transmission line. This was a motivation because the current flowing to and from Obib substation can easily be verified using ohms law due to the simplicity of the circuitry around the Obib substation. The presence of one transmission line created an interest to collaborate with SANSA and they installed 2 magnetotelluric meter units under the transmission lines to measure the magnetic field under the transmission line which can be used to calculate GICs in the line. In addition, the Obib substation is also among the substations with high GIC magnitude in the network.

GIC measurements were done on a 400 kV-66 kV transformer 1. The Obib single line diagram is shown in the Appendix.

5.11 Equipment calibration

It was crucial to ensure that the measurement devices are properly calibrated to take accurate measurements. The data logger and the current and voltage modules used were already calibrated by the manufacturer (NI). Whereas, the current probes were calibrated manually by the author by using a hand held button on the Hall-effect transducers.

With the technical assistance of NamPower personnel, the magnitudes of the signals measured from the current probes were compared to the magnitudes obtained using a fluke multi-meter to verify that the Hall-effect transducers are properly calibrated.

For continuous power supply to the current probes, an AC-DC converter was used. The transducers were first calibrated before the battery supply to the transducers was changed to the converter. It was found that the CP30 current probe calibrated properly when it was being supplied from either the battery or from the AC-DC converter. However, the H20.3C current probe was unable to calibrate properly when it was supplied from the AC-DC converter. During the calibration process, the signal being measured by the Hall-effect transducer was also compared at the point of connection (i.e. at the Hall-effect transducer) to that at the point of measurements (i.e. at the data logger). This was done to ensure that there is minimal interference on the cables used to transmit the signals especially because the cables might be running close to HV cables.

An investigation was done to find out why the H20. 3C could not calibrate properly when the AC-DC converter was employed. Possible reasons for this could be associated with the ripple from the power supply or the interference on the cabling used or the *sneaky* earth caused due to grounding of the cabling used. The last two reasons were tested by comparing the measurements at the point of measurements with those at the point of connection and the signals were found to be the same. To investigate the possible reasons of ripples affecting the measurements, it was found that the power supply was indicated to have 120 mV p-p ripple. The magnitude of the ripple might be large enough to cause distortions in the measurements because the output sensitivity of the H20. 3C is 1 mV/A or 10 mV/A. To avoid the possible problems with distortions, four parallel 9 V large batteries were used for the H20. 3C to ensure that it is calibrated properly. After employing the 9 V batteries in parallel, we were able to take good measurements with the H20. 3C compared to when the supply was an AC-DC converter.

5.12 Geomagnetic field data

Real time geomagnetic field data were obtained from the Hermanus Magnetic Observatory (HMO) which is located in Hermanus, a town on the Southern Coast of South Africa. Field and station magnetometers are used to collect the data and appropriate algorithms are applied to calculate regional electric field assuming uniform magnetic field and uniform ground conductivity

5.13 Chapter Summary

A detailed description of the proposed GIC equipment was shown including the specifications and how the measurements were be taken.

A laboratory prototype used to test the equipment set-up was described and tested successfully. Results obtained using the proposed GIC equipment were compared to the readings obtained using the Yokogawa Power Meter and a good agreement was found.

Two sites were chosen for GIC measurements namely the Ruacana and Obib substations and installations were done successfully.

The next step is to perform preliminary data analysis and thereafter compare the measured results with calculated results.

Chapter 6

GIC measurements in the Namibian transmission network

This chapter presents actual measurements taken during the course of the dissertation. Two methods used for analysis in this dissertation are the FFT method and filtering by averaging. Measurements from geomagnetically quiet days were analysed. Furthermore, measurements from a geomagnetically storm day were compared with modelled results obtained, using the Nodal Admittance method assuming a uniform plane wave and uniform ground conductivity. Comments were made on the results. Possible sources of errors in the measured results are presented and ways to eliminate the effects caused due to the errors are also discussed.

6.1 GIC measurement equipment Installations

After the complete proposed equipment set-up was tested successfully, three measurement units were installed successfully in the Namibian transmission network, one at the Obib substation and two at the Ruacana substation. The measurement units were in operation from 22 July 2013 to date. **Figure 6-1** shows where the neutral Hall-effect transducers were connected on the primary side of the transformer.

Figure 6-1: Transformer neutral bushing

Hall-effect transducers measure both AC and DC currents and thus the neutral current recorded will be a combination of mainly the GIC and the 50 Hz neutral current. The neutral

data is then filtered offline to remove high frequency components and hence the output is expected to correspond to a GIC only.

There has not been any severe geomagnetic storm between the 22nd July 2013 and 1st October 2013 since the installation of measuring equipment was completed. This entire period was regarded as a magnetic quiet period. There was a double coronal mass ejection (CME) predicted that was supposed to reach the Earth between the 19th and 20th August 2013, however it was not felt on the Earth and it was assumed to have either missed the earth completely or it is late according to *www.spaceweather.com*. Another minor CME was predicted to reach the Earth between the 23rd and 24th September 2013; however it was not visible in the data. The biggest solar storm experienced since the equipment were installed was on 2nd October 2013 corresponding to a K (HER) =7 index.

The results presented in this chapter are composed mostly of geomagnetically quiet days and the results of the highest CME experienced during the course of the measurements.

The data logger was specified to take continuous sampling and a total of 96776 samples per minute.

6.2 Preliminary results

After the installations at the two measurement sites were completed, a Fluke multi-meter was used to show what the AC component and DC component is composed in the neutral current. It was found that approximately 6 A magnitude of AC component was flowing in the neutral at Obib substation and Ruacana substation. This magnitude brought about questions on whether or not it was significant to pose any threat to the transformer and if so, why is the protection scheme not triggered when the 6 A flows in the neutral. To investigate this further, it was discovered that since the neutral transducers are connected on the primary side of the transformer neutral, it was found that the neutral CTs used on these transformers have a ratio of 1600:1 A. This indicates that the 6 A primary current correspond to only 3.75 mA flowing in the secondary side of the transformer which is negligible for the protection scheme to be triggered.

Under normal conditions, there should be approximately zero AC current flowing in the neutral. Any non-zero AC currents present in the neutral might be associated with the transmission line not transposed or the presence of capacitive currents. It was found that the 400 kV line feeding the Obib substation is un-transposed which could explain the presence of the 6 A magnitude AC current in the neutral. However, the transmission line feeding the

Ruacana substation is transposed which does not explain the presence of a non-zero AC current in the neutral.

The Ruacana substation has four identical generation transformers however, in the winter season, the operators only run at most two generation transformers. During the first stage of data analysis it was found that, when the transformers were offline and isolated from the entire network, the neutral Hall-effect transducers were measuring a DC current of the same magnitude as when the transformers were online. From circuit theory if a transformer is offline and isolated from the network, there should not be current flowing in the transformer phases or in the transformer neutral. For this reason, it was later decided to omit the Ruacana results and only present the Obib substation results in this dissertation. The investigation of the Ruacana installation will be performed outside the scope of this dissertation.

It was also discovered that the voltage data for Obib substation was heavily distorted and can thus not be used in the analysis. Therefore, only the Obib neutral current and two current phases will be used in the analysis.

6.3 FFT analysis for the 24th July 2013

Geomagnetically quiet days are characterised as days with K (HER)-index less than 5. In this section, results of the 24th July 2013 corresponding to a geomagnetically quiet day are shown. **Figure 6-2** shows a sample of the neutral current waveform over half a second period for the 24th July 2013. The neutral current ranges from -10 A to 10 A. From **Figure 6-2**, it can be seen that the waveform is unbalanced and further analysis need to be performed to investigate what harmonic components are contained in the neutral current waveform.

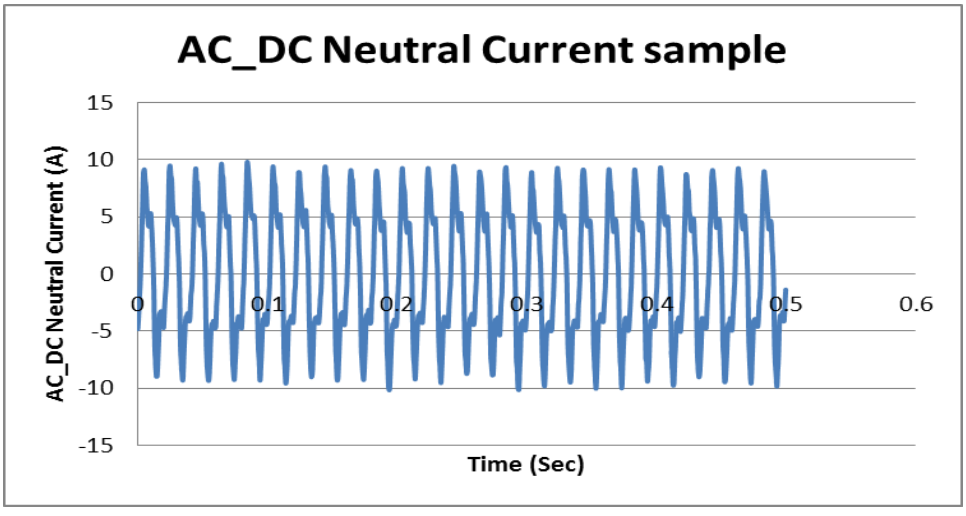

Figure 6-2: AC_DC Neutral Current waveform indicating an unbalance in the Neutral Current

To investigate the presence of harmonics in the neutral current, an FFT analysis was performed. **Figure 6-3** shows harmonic magnitudes composed in the neutral current. It can be seen that there is a strong unbalance indicating a dominant 1st harmonic and a significant 3rd harmonic compared to the 2nd and 4th harmonic. The remaining harmonics from the 5th harmonic are small compared to the first 4 harmonics.

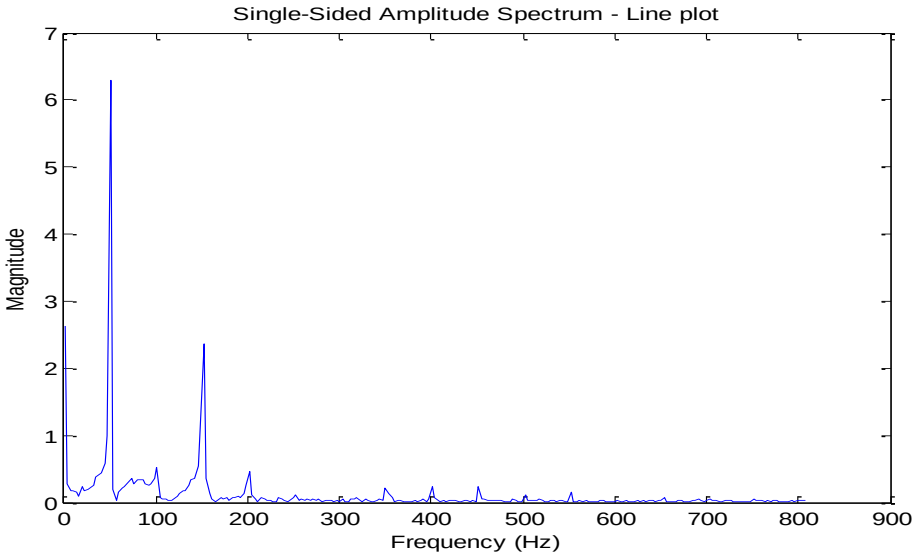

Figure 6-3: FFT analysis for the 24th July 2013

6.4 Results of geomagnetically quiet days from July – October 2013

To extract the DC flowing in the transformer neutral, the data recorded was filtered using a 1-minute average. Some of the 1-minute average results for geomagnetically quite days are shown in **Figure 6-4** and **Figure 6-5** below. All the days shown are categorised as geomagnetically quiet days because they fall on days with the K (HER)-index less than 5.

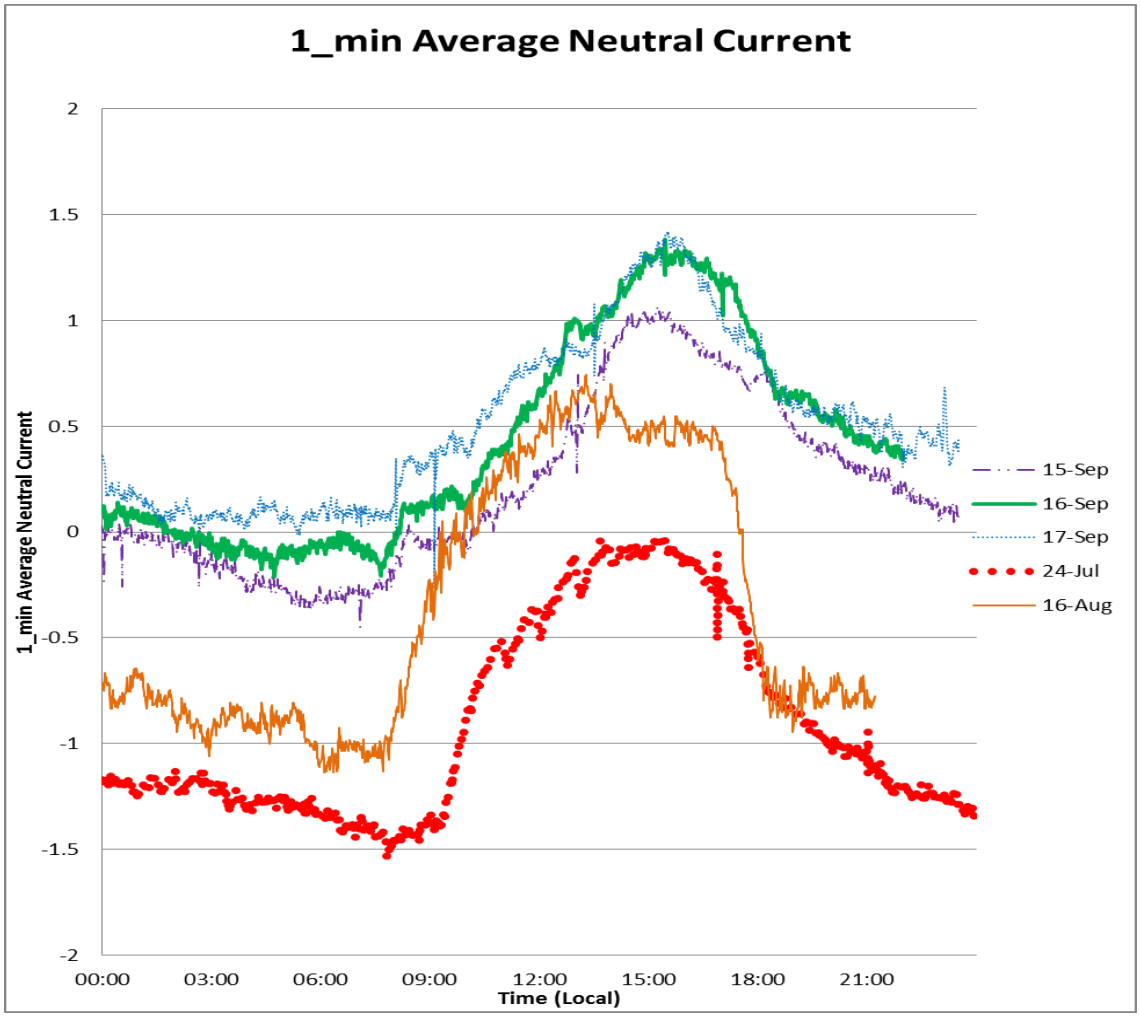

Figure 6-4:1_min Average Neutral Currents for different geomagnetically quiet days

From **Figure 6-4**, it appears as though the neutral current for the different days are approximately constant from 12 am to 7 am. This could be interpreted as caused by calibration drift of the Hall-effect transducer's DC offset. However, looking at the results for the entire day, it is visible that the Hall-effect transducer is measuring a variation ranging from -1.2 A to 1.4 A for the days shown in **Figure 6-4.**

More readings from geomagnetically quiet days recorded in October are shown in **Figure 6-5.**

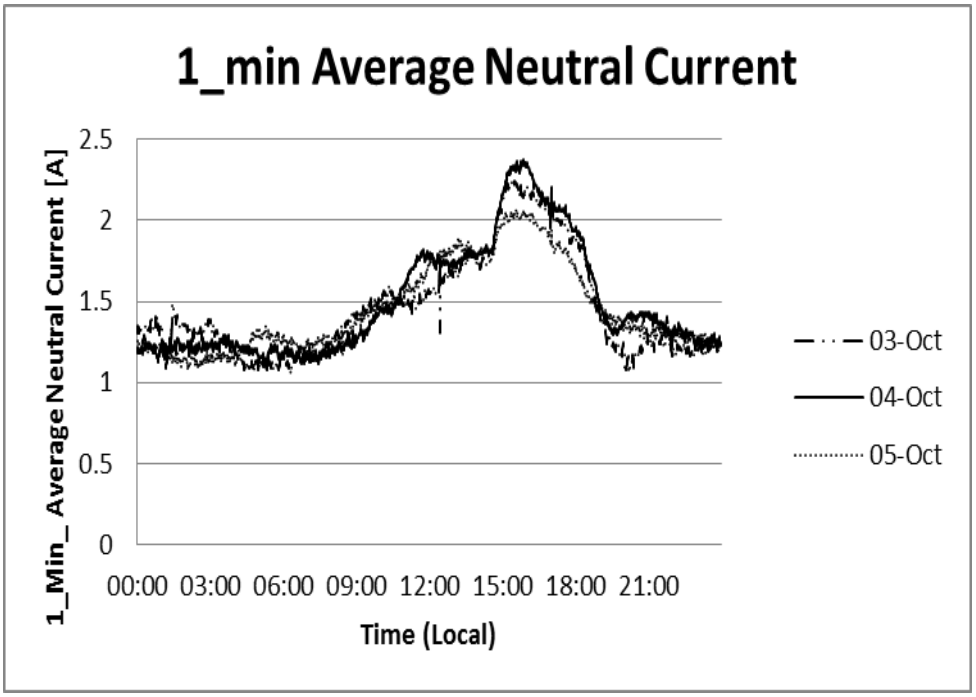

Figure 6-5: 1_min Average Neutral Current for different days in October 2013

A similar trend is seen in **Figure 6-5** however the 1-min average neutral current in October 2013 appear to be higher than that of days between July, August and September of 2013.

From **Figure 6-5**, a similar trend is seen which appears to rise between 8 am to 3 pm and fall from 3 pm till 12 am. The trend shown appears to be similar to that of the diurnal temperature variation. Further investigations need to be shown for a geomagnetically storm day to observe whether the variations of the neutral current caused due to the solar storm can be seen from the measurements.

The Ruacana substation is an underground station and the generation transformers which were used for GIC measurements are also underground and not exposed to direct sunlight. However, the Obib substation is an outdoor station and the transformers are exposed to direct sunlight. The neutral Hall-effect transducer at Obib substation is also installed outdoors on the transformer neutral conductor and is exposed to direct sunlight. The sensitivity of the Hall-effect transducers could be affected by the daily temperature variation which might explain why the Obib results observed follow a diurnal temperature variation. The Ruacana data demonstrated to be inconsistent and could not be used to test the apparent temperature variation theory.

6.5 Results of a geomagnetic storm day for the 2nd October 2013

From July to September 2013, there has not been a significant CME event. Measurement results from geomagnetically quiet days appear to be sensitive to daily temperatures and thus were inconclusive to indicate how much GIC is flowing in the network on a particular day. Further measurements were required for a relatively strong CME event to be able to distinguish between variations caused due to temperature and those due to a CME event.

During a CME, more variations are expected in the measured results due to the CME compared to the variations due to temperature because the temperature variation during the day is gradual. After the CME, it will be possible to obtain measured data to compare and validate the Nodal Admittance method. As a result of a possible temperature sensitivity observed in the measurements, a temperature compensation technique will be applied before comparing the measured results to the modelled results using the Nodal Admittance technique.

There was a strong geomagnetic storm that affected the Earth on the 2nd October 2013 corresponding to K (HER) =7 index. In this section, the GIC measurements of the 2nd October 2013 will be analysed and compared with measured results of the geomagnetically quiet days. This was performed to investigate whether there is a distinct difference in the variations of the results between a geomagnetically quiet day and a geomagnetically storm day. The geomagnetic storm of the 2nd October 2013 lasted for the first half of the day.

One of the research questions was to investigate how accurately the results obtained using the simulation technique correlates with measured results. The Nodal Admittance method was used to modelled the predicted GICs in the network and thereafter compare with measured results. The magnetic field data used in the calculations were obtained from SANSA using the standard based on published models. The data was measured the Keetmanshoop magnetic observatory (KHM) in Namibia with coordinates 26.320^0S, 18.060^0E, which is the closest observatory to the Obib substation. The electric field data for the entire network was calculated using M=10 and a plane wave model assuming uniform ground conductivity for the entire network.

GIC results obtained using the Nodal Admittance technique corresponds to GICs flowing in the grounded neutral conductors of all the grounded equipment in the substation mainly transformers and reactors. In this dissertation, reactors are approximated to have a larger ground resistance compared to transformers and thus the neutral current flowing in the

reactors will be much smaller compared to that flowing in the transformers and can thus be ignored. In addition, modelled GICs for Obib substation will the divided equally among the two transmission transformers. Only one transformer was used for GIC monitoring and hence the measured GIC will be assumed to be the same for both of the two transformers since they are identical.

Figure 6-6 shows a comparison between the CME day (2nd October 2013) to the geomagnetically quiet days corresponding to approximately the same average daily temperature.

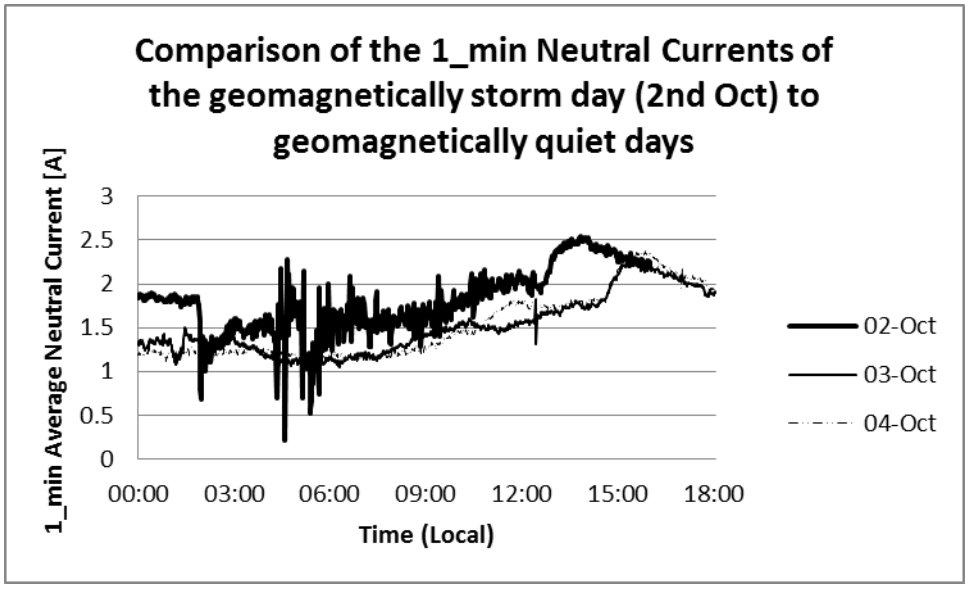

Figure 6-6: Comparison of the 1-min Average measured Neutral Currents of the geomagnetically storm day (2nd Oct) to the geomagnetically quiet days of a similar daily average daily temperatures

From **Figure 6-6**, a visible rapid fluctuation in the 1-min Average Neutral Current for the 2nd October compared to the solar quiet days is observed.

From the results, it was observed that the data for the geomagnetically quiet days might be highly dependent on the temperature, it was first necessary to compensate for the temperature dependency of the data. This was done to ensure that the results will only display the fluctuations resulting from a CME corresponding to GICs. To do this, a temperature compensation technique was applied on the CME day's data to remove the temperature dependency. This was done by removing average GICs for geomagnetically quiet days those approximated to have the same temperature as the CME day. This approach also assumes that the Hall-effect transducer was measuring the same offset on both quiet and solar geomagnetic days.

Figure 6-7 shows a comparison between calculated and measured results flowing in the Obib substation. A temperature compensation technique was applied on the measured results using the average of the geomagnetically quiet days corresponding to the 3rd, 4th and 5th October 2013. The resultant GIC for the 2nd October was obtained by subtracting the average neutral current of the solar quiet days for the 3rd, 4th and 5th October from the measured results of the 2nd October.

The 2012 Namibian network parameters used in the model, to calculate the predicted GIC flowing in the network, are shown in the appendix. It was assumed that there were no major changes to the network between 2012 and 2013. The exact coordinates for the substations are confidential NamPower data and they were excluded from the appendix. The relevant parameters used for GIC calculations are the substation coordinates, line lengths, the number of transformers at the substation, the nodal admittance for the neutral conductors at each substation, line admittances and the electric field data obtained from SANSA. The GIC was calculated using the Nodal Admittance method as described in Chapter 4.

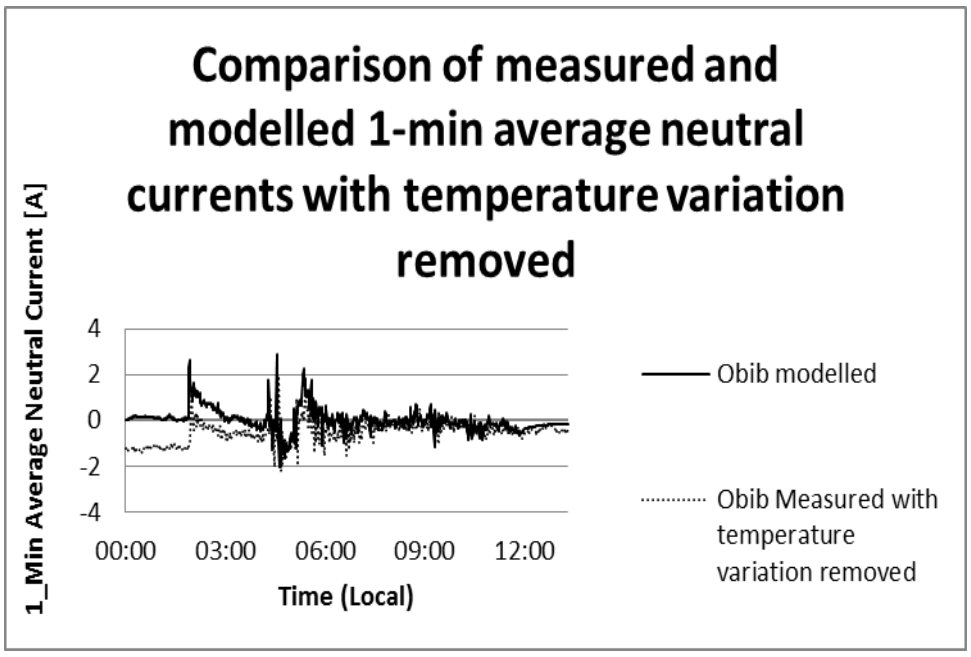

Figure 6-7: Comparison of 1-min Average neutral currents using a temperature compensation technique

From **Figure 6-7**, there exist good correlations between measured and modelled results for the periods of rapid fluctuations compared to the periods of slow fluctuations. This can be attributed to various factors such as the approximations made on the temperature compensation technique.

Comparing the measured with the modelled results in **Figure 6-7**, there appear to be an offset of 1.3 A between the two results. This offset can be attributed to the temperature differences between the 2nd October and the geomagnetically quiet days used to remove the temperature variations from the measured results. An analysis was performed to investigate the result of removing the 1.3 A offset to investigate if there is an improvement in the correlation of the results. This is demonstrated in **Figure 6-8** below.

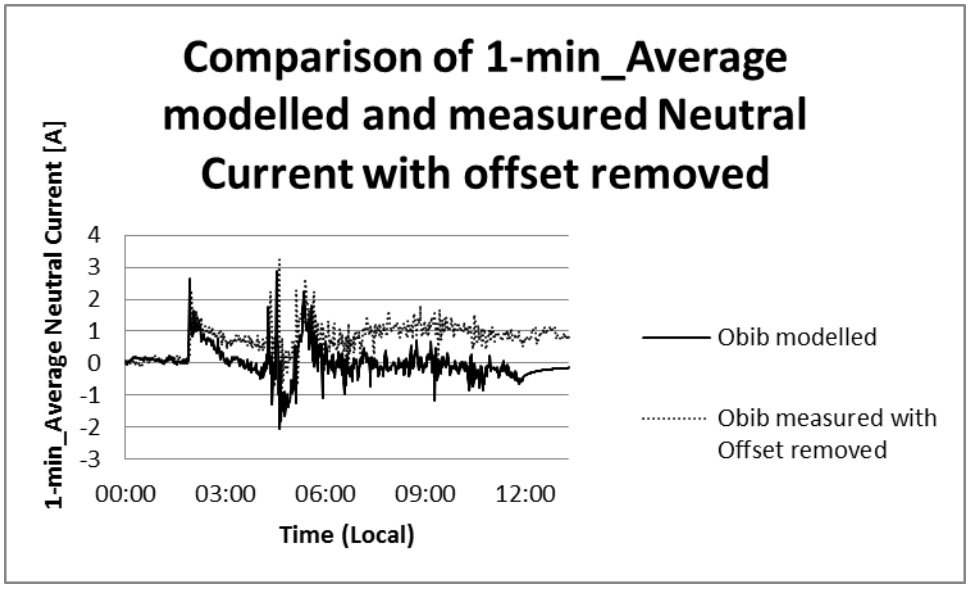

Figure 6-8: Comparison of 1-min Average neutral currents with an offset of 1.3 A removed

Figure 6-8 shows that removing the offset improved the comparison for slow fluctuations while the rapid fluctuations were worsened.

Other factors which could explain the difference between the measured and the modelled results can be attributed to the assumption of using the uniform plane wave method, uniform ground conductivity method and assumptions made about the frequency components of the resistance in the network.

6.6 Exposure of the entire network

The last research question required to test the hypothesis of this dissertation is to investigate what is the exposure of the Namibian network to GICs. In this section, the exposure of the network is shown.

To investigate the exposure of the Namibian network during the CME of the 2nd October 2013, the magnetic field data for the 2nd October 2013 from the Keetmanshoop observatory was used for the entire network assuming uniform plane wave and uniform ground conductivity using M=10. **Figure 6-9** to **Figure 6-11** shows the predicted GIC flowing in some of the substations.

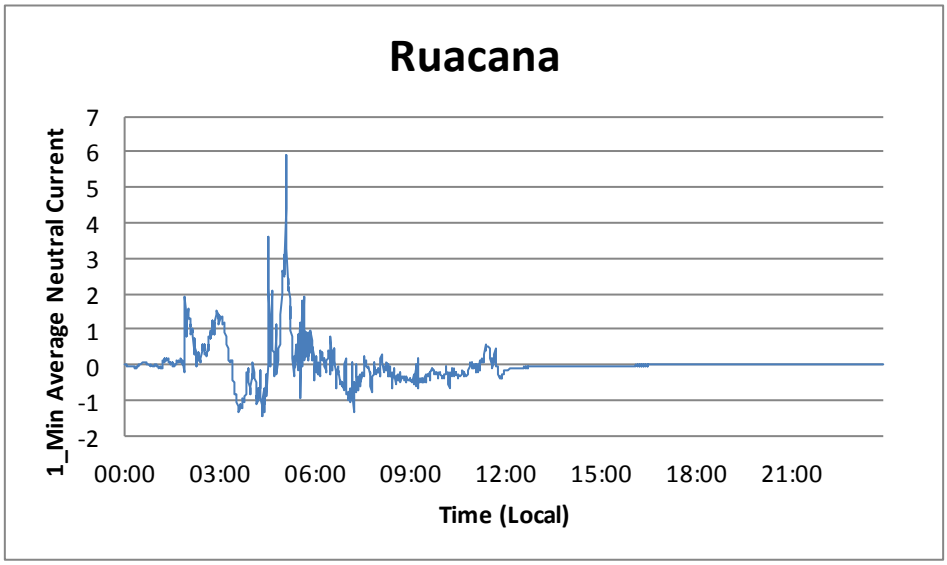

Figure 6-9: Modelled GIC for Ruacana substation

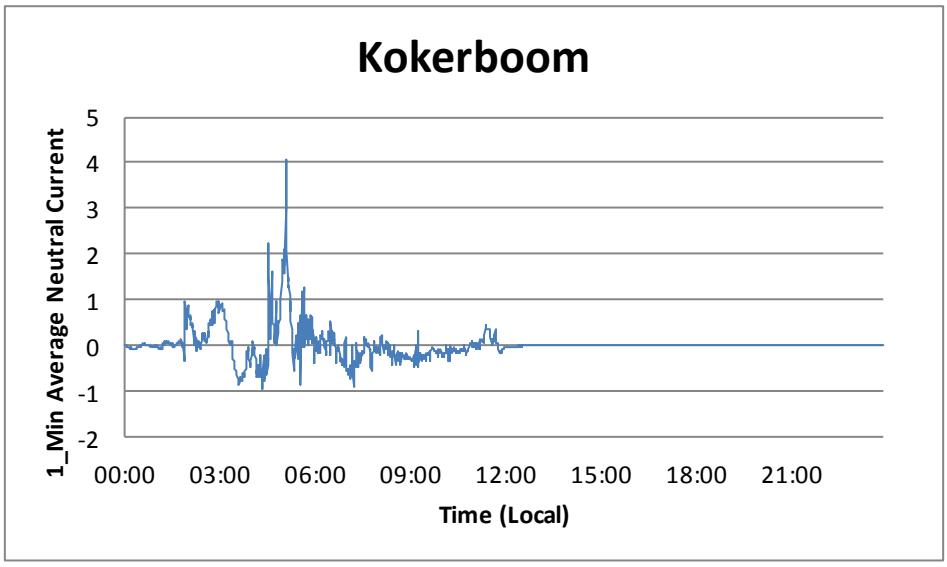

Figure 6-10: Modelled GIC for Kokerboom substation

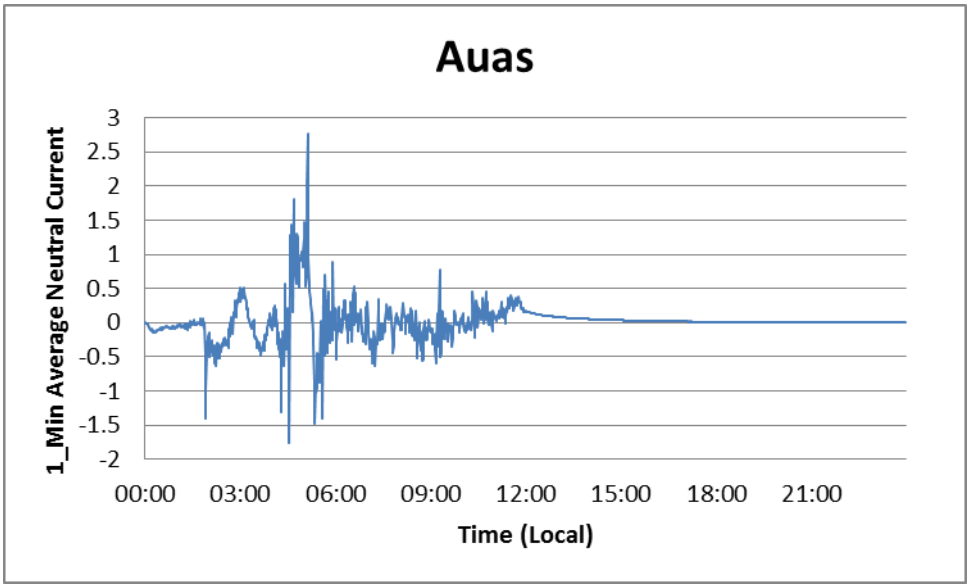

Figure 6-11: Modelled GIC for Auas substation

Table 6-1 shows maximum modelled GIC magnitudes for all the substations in the network. Aries substation was found to have the highest GIC magnitude, however Aries is part of the South African network. Therefore, from the Namibian network, Ruacana was found to have the highest GIC followed by Kokerboom, Auas and Obib substation. The remaining substations showed GIC maximums of less than 3 A.

Table 6-1: Calculated GICs for the entire network showing maximum absolute GICs

2012 Namibian transmission substations	Absolute Max GIC [A]
Aggeneis	2.1
Aries	8.9
Kokerboom	4
Ruacana	5.8
Omburu	1.3
Auas	3.7
Van Eck	0.8
Khan	1.2
Trekkopje	0.8
Rossing	0.2
Walmund	0.65
Kuiseb	1.1
Gerus	1.1
Otjikoto	0.8
Osona	0.25
Hardap	0.45
Obib	3
Karas	0.27
Harib	0.6
Oranjemond	2.6

6.7 Capacitive current observations

An analysis was performed to investigate whether the AC current flowing in the transformer neutral is capacitive or not. Since the voltage data was observed to be inconsistent, the capacitive current analysis will be investigated using phase current data. Only two phase currents were measured in this dissertation and therefore the third current was calculated using Kirchhoff's Current Law (KCL).

A sampling frequency of 1.613 kHz was used resulting in 32.26 samples per 50 Hz cycle. A dominant 3rd harmonic was observed in the neutral current as presented in section 6.3. This was first removed from the two phase currents before calculating the third phase. The 3rd harmonic was removed by applying a moving average over 11 samples. From section 6.3, it was shown that the remaining harmonics in the neutral current are small relative to the 3rd harmonic and thus after removing the 3rd harmonic, the resultant signal can be approximated to be a 50 Hz signal only.

Figure 6-12 shows a portion of phase currents as measured on a geomagnetically quiet day (24th July). Only the blue and red phase were measured and the yellow phase was calculated using KCL.

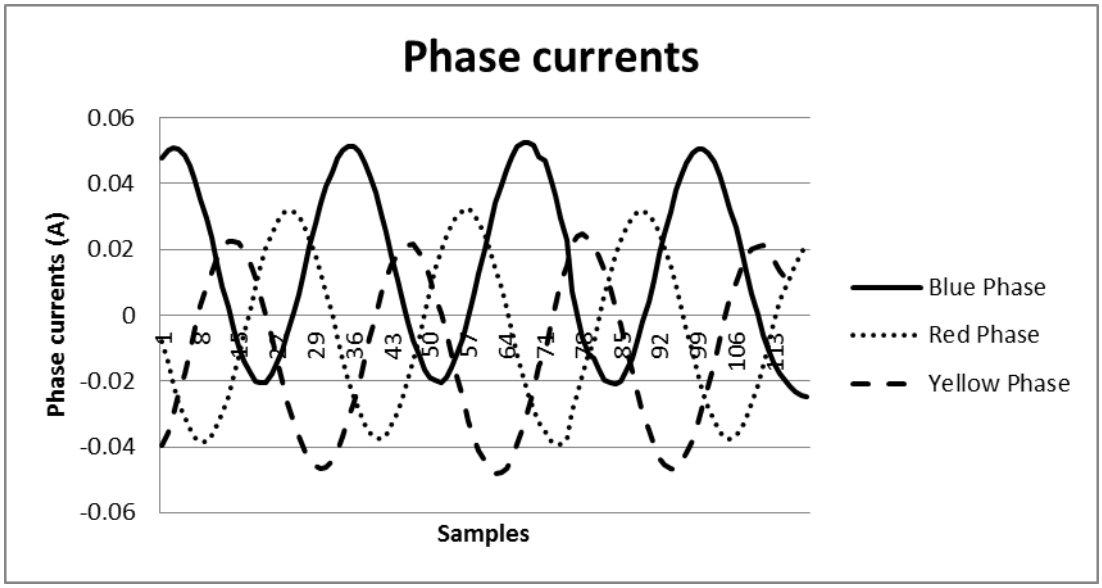

Figure 6-12: Phase currents

From **Figure 6-12,** a high asymmetry about zero is observed in the red and blue phase while the asymmetry in the yellow phase is much smaller compared to the other two phases. This zero-shift can be attributed to the calibration drift of the Hall-effect transducers which could be caused by the use of the DC converter as a power source. Due to the inconsistencies in

the current phase's data, it is not possible to conclude the investigation of the capacitive current analysis and further investigations are necessary to conclude this investigation.

6.8 Frequency fluctuations in the 1-4 Hz band

An analysis was done to investigate whether there are fluctuations in the 1-4 Hz band of the neutral current data. This investigation was done as another way of smoothing out the high frequency variations in the measured current sampled at high frequency. An FFT analysis was performed, for each minute for a duration of 5 minutes for two quiet days namely, for the 16th August and 3rd October and a storm day for the 2nd October. The specified days were chosen since the main purpose of this investigation is to analyse the 1-4 Hz fluctuations in the geomagnetically quiet days and geomagnetically storm days.

Figure 6-13 to **Figure 6-22** demonstrates the FFT analysis of the neutral current on geomagnetically quiet days for a duration of 5 minutes zoomed in around the 1-4 Hz region.

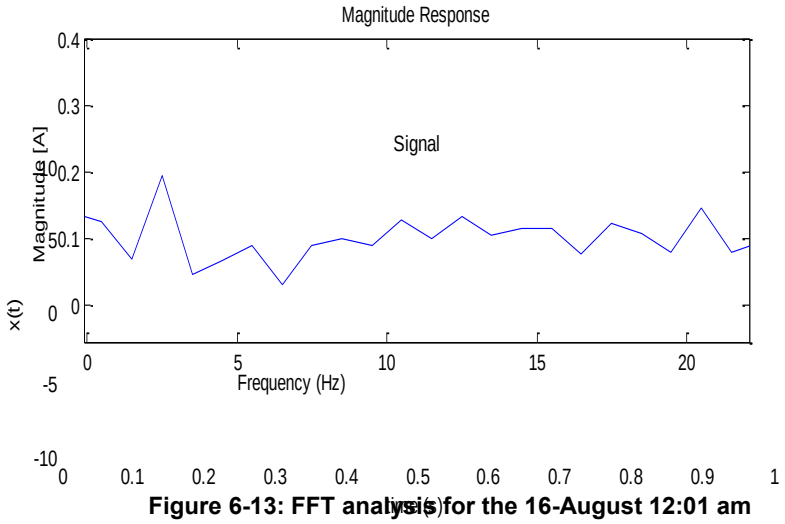

Figure 6-13: FFT analysis for the 16-August 12:01 am

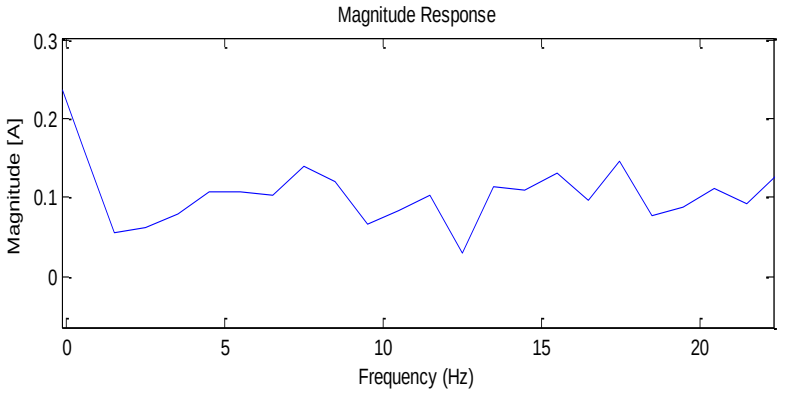

Figure 6-14: FFT analysis for the 16-August 12:02 am

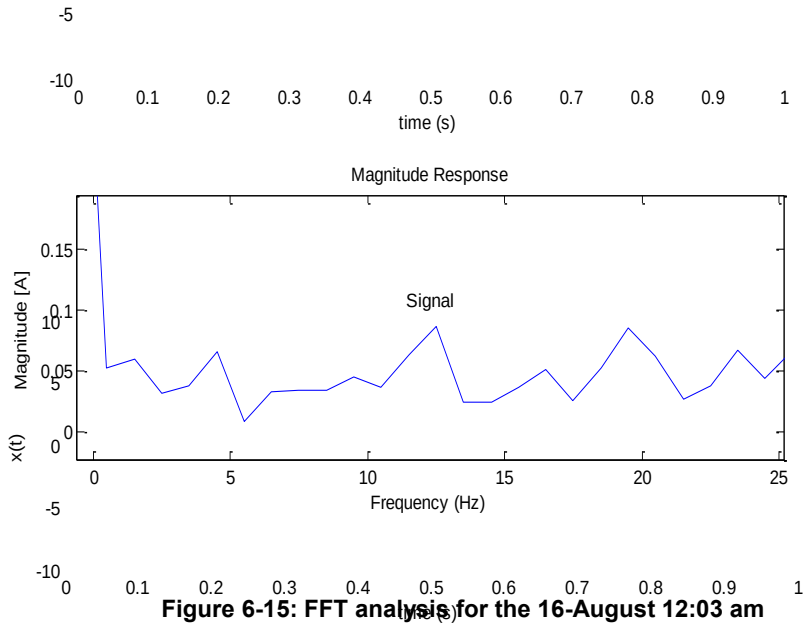

Figure 6-15: FFT analysis for the 16-August 12:03 am

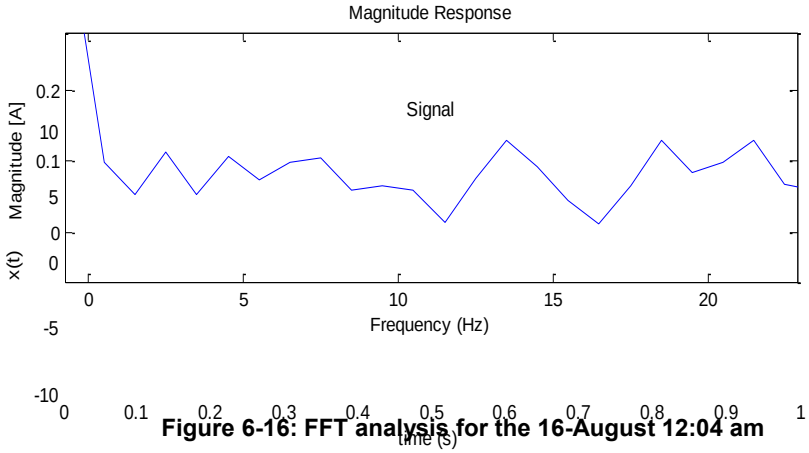

Figure 6-16: FFT analysis for the 16-August 12:04 am

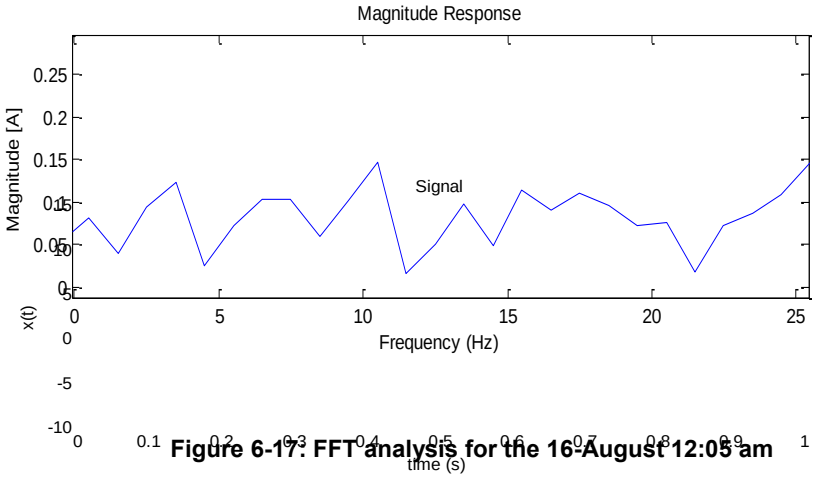

Figure 6-17: FFT analysis for the 16-August 12:05 am

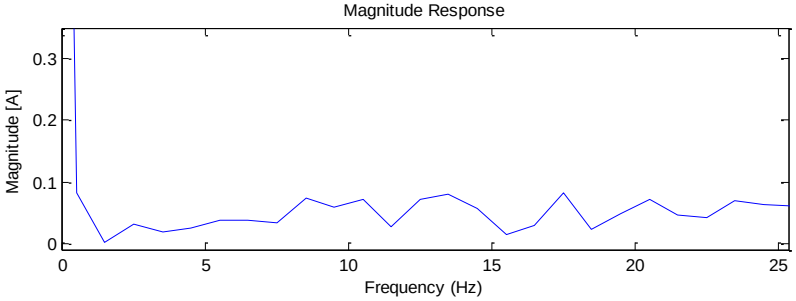

Figure 6-18: FFT analysis for the 3-October 12:01 am

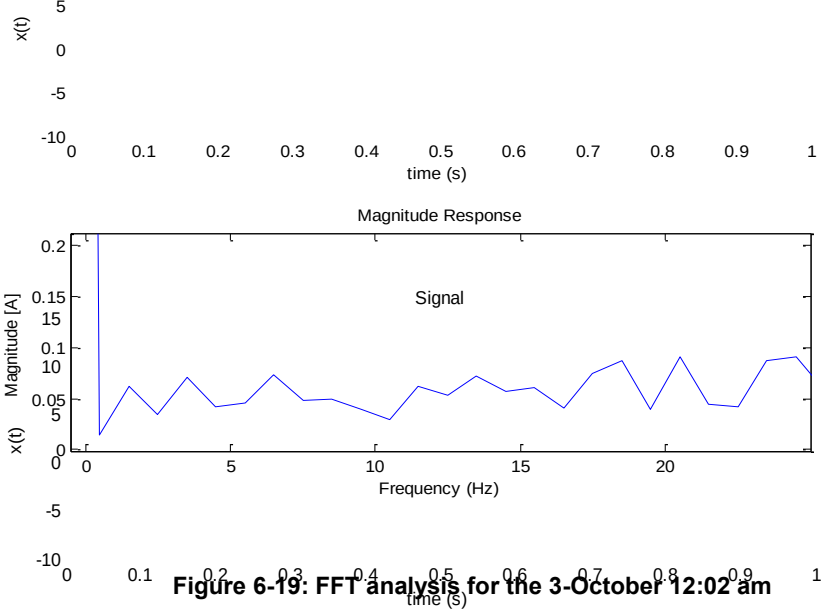

Figure 6-19: FFT analysis for the 3-October 12:02 am

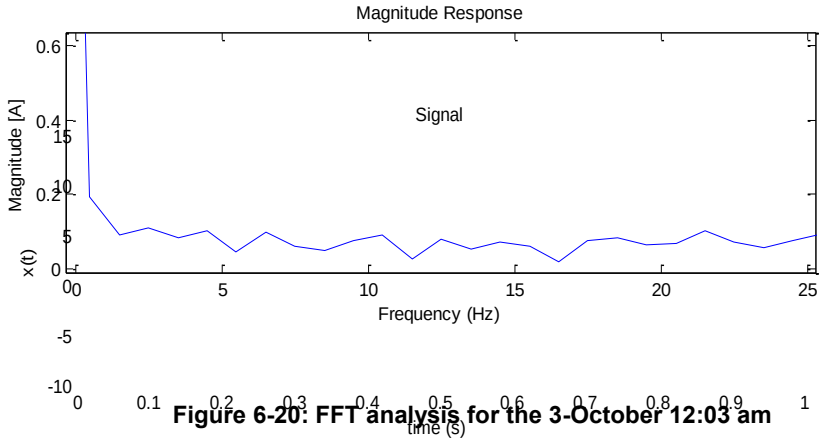

Figure 6-20: FFT analysis for the 3-October 12:03 am

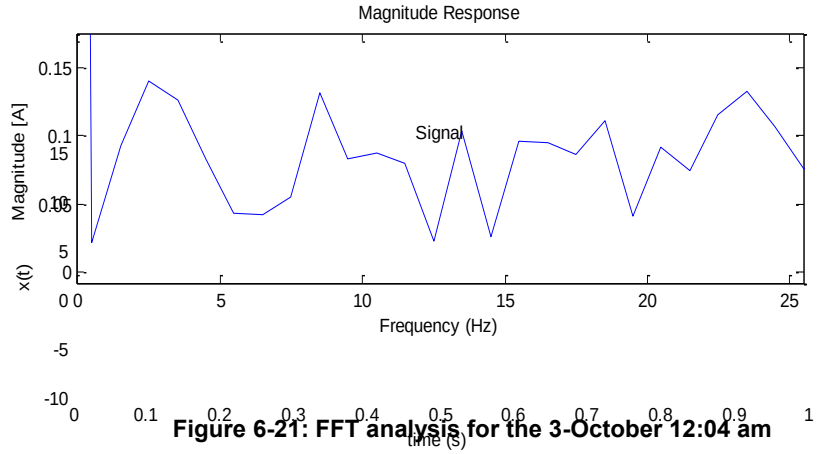

Figure 6-21: FFT analysis for the 3-October 12:04 am

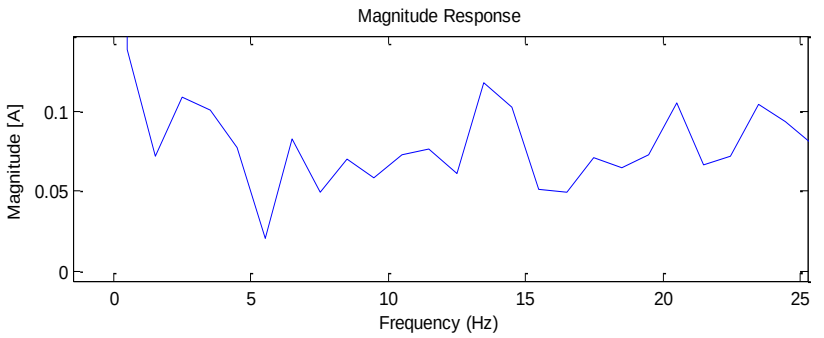

Figure 6-22: FFT analysis for the 3-October 12:05 am

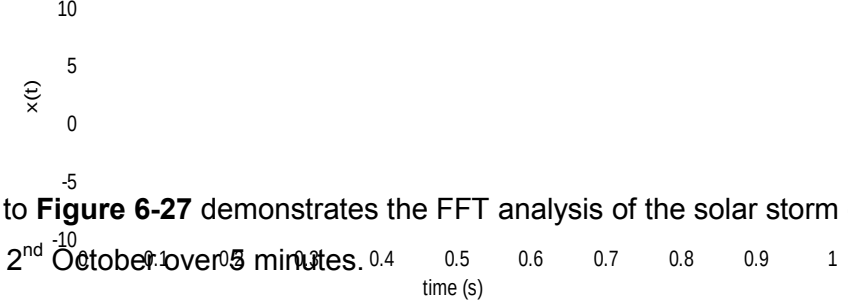

Figure 6-23 to **Figure 6-27** demonstrates the FFT analysis of the solar storm day which took place on the 2nd October over 5 minutes.

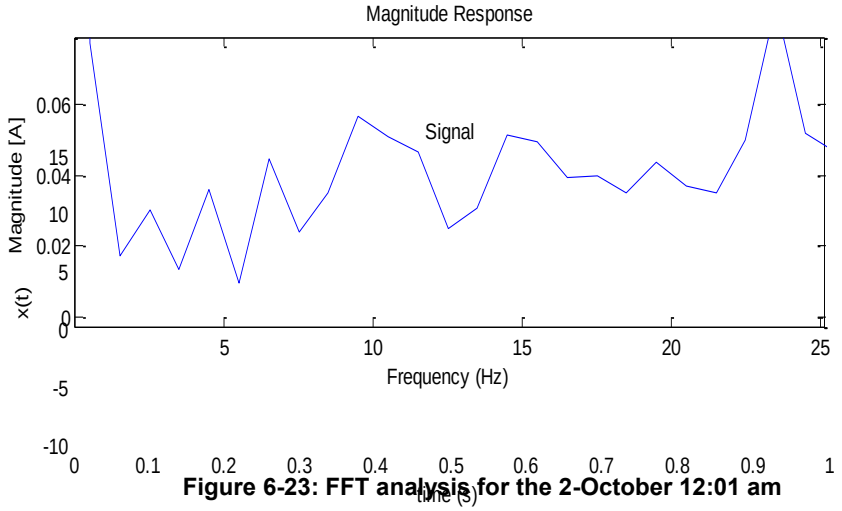

Figure 6-23: FFT analysis for the 2-October 12:01 am

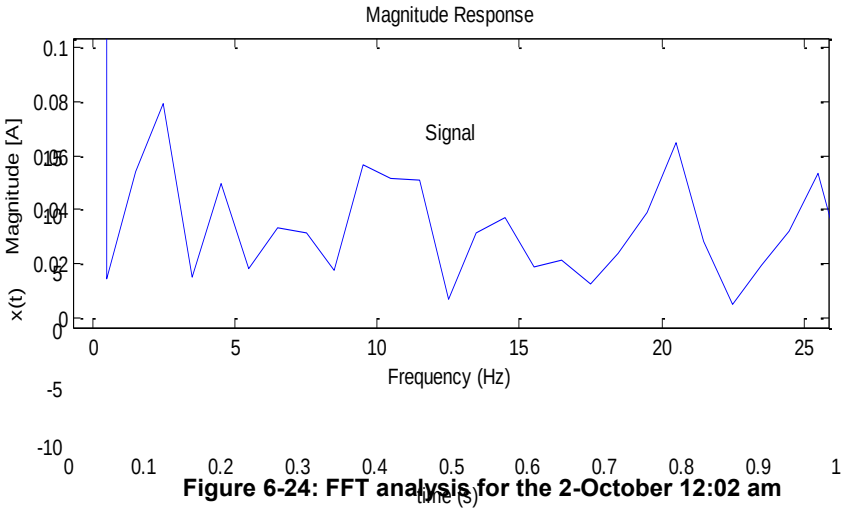

Figure 6-24: FFT analysis for the 2-October 12:02 am

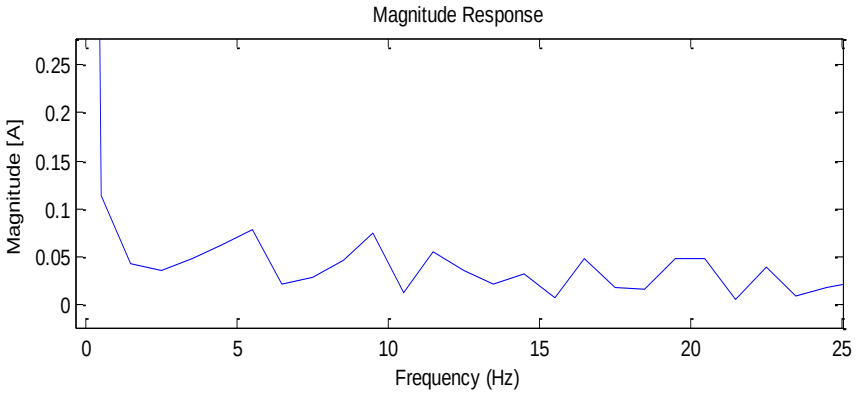

Figure 6-25: FFT analysis for the 2-October 12:03 am

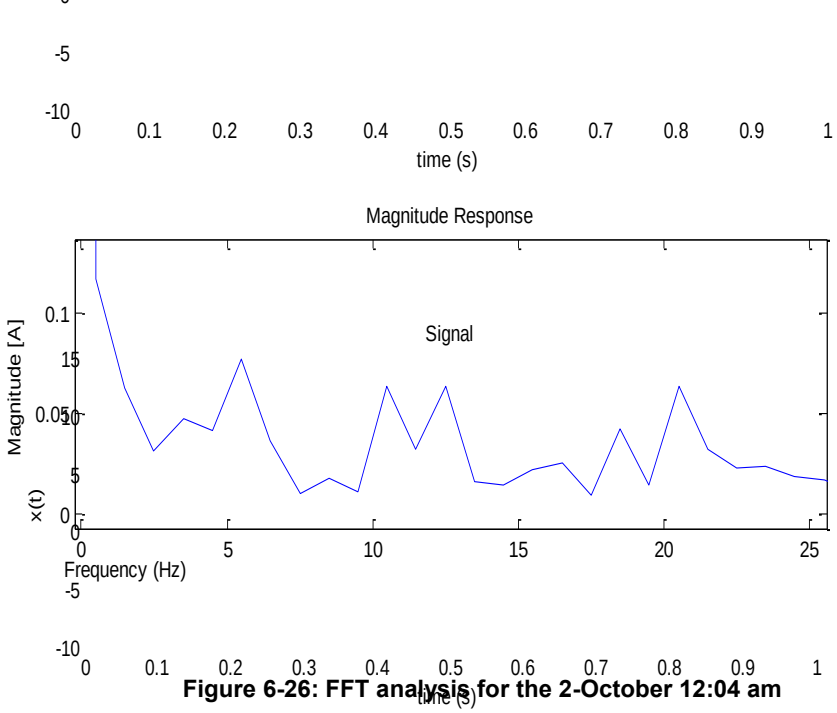

Figure 6-26: FFT analysis for the 2-October 12:04 am

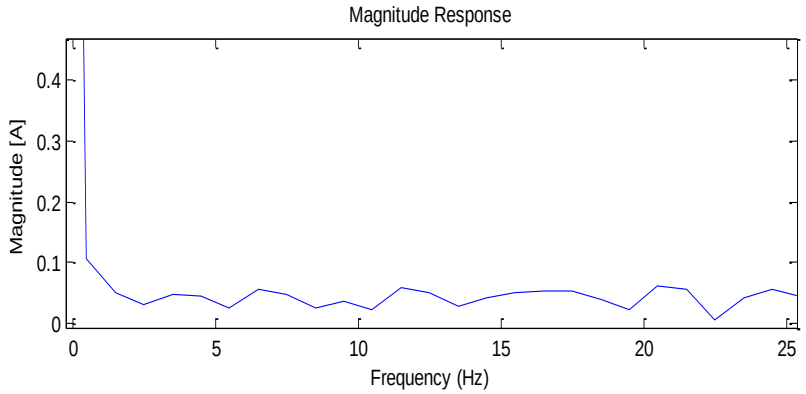

Figure 6-27: FFT analysis for the 2-October 12:05 am

From **Figure 6-12** to **Figure 6-**27, a pattern appeared to emerge in the 1-4 Hz band which was visible in both the geomagnetically quiet days and during the geomagnetically storm day. The low frequency response was not always evident in the data. This could point to another characteristic of the NamPower transmission network or a characteristic of transmission networks possibly sub-synchronous resonance since the phenomenon has been reported on the Namibian network. More investigations are required to understand this characteristic and also see if it correlated with GMDs.

6.9 Power factor investigations

The power factor is given by the ratio of P/S where P is the active power and S is the apparent power. From literature, it is observed that in the presence of GICs, the power factor is decreased because there is an increased in the apparent power. The active and apparent power calculations are done using three phase current and voltage waveforms. In this

dissertation, only two phase currents and three phase voltage waveforms were measured. The voltage waveforms were highly distorted and an additional phase current needed to be calculated to be able to calculate the power factor. For this reason, it was not possible to analyse how the power factor was affected during geomagnetically quiet days compared to geomagnetically storm days.

6.10 Scope and limitations

The scope of this dissertation includes investigating the best equipment for GIC measurements and thereafter installing the equipment in the Namibian transmission network. Before installing the equipment in the network, the proposed equipment set-up was tested in the laboratory on a published laboratory set-up. Only two sites were chosen in the network for GIC measurements and the installation was completed successful on 3 transformers, one at Obib substation and two at the Ruacana substation.

The development of the Nodal Admittance calculation technique and the FFT technique was not covered in this dissertation, it was merely applied. To illustrate basic application of the Nodal Admittance method, simple circuits were studied exposed to different electric fields to investigate how GICs flow under different conditions. Furthermore, this dissertation does not cover the effects of GICs on the transformer.

From the time the equipment was installed in the network, there was only one strong CME reported which took place on the 2nd October. Measurements taken on geomagnetically quiet days were not conclusive to indicate how well the measured results compare with modelled results. Moreover, measurements indicate a possible temperature variation dependency which will be possible to eliminate from the data using measured data from a solar stormy day to be able to measure the variations due to CME compared to variations due to temperature using temperature compensation techniques. The temperature compensation technique made use of averaged geomagnetically quiet day' results assumed to have the same average daily temperature. Further work still need to be done to ensure that the temperature compensation technique is improved.

6.11 Possible sources of errors

- Changes in the network configuration such as line trips etc.
  For the duration of the research the network was assumed to remain constant. This could lead to errors in the modelled results especially if a major line is out of service or during substation shutdowns.
- Only limited number of sites for magnetic field data

The Nodal Admittance calculation technique used in this dissertation was used under the assumption that there is a uniform electric field for the entire network however, it was found in literature that a uniform electric field does not improve the error between measured and modelled results. Having a large number of magnetic field data sites will reduce the error between the calculated and measured results by applying the Spherical Elementally Current Systems (SECS).

- Temperature sensitivity of the Hall-effect transducers
  Given that the Hall-effect transducers might be highly sensitive to temperature variations, the neutral current being measured cannot be compared to the calculated results without applying a temperature compensation technique. Care must be taken when applying the temperature compensation technique putting into consideration the temperature variations for the different days.

6.12 Chapter summary

After successfully installing the GIC measurement devices, measured results were shown and discussed. Some inconsistencies were found in the Ruacana neutral readings indicating a presence of a DC current flowing in the neutral when the transformers were offline and isolated. As a result, the Ruacana readings were found to be in-accurate and were omitted in the dissertation. Further investigations are needed on the Ruacana installation, however it is out of the scope of this dissertation.

Furthermore, a non-zero AC neutral current was observed in the Obib substation data and was indicated to be caused by the presence of an un-transposed transmission line. FFT analysis of the neutral current showed a significant unbalance and a high 3^{rd} harmonic content compared to 2^{nd} and 4^{th} harmonic. Measurements from geomagnetically quiet days show a similar trend to that of the temperature diurnal variation. It was necessary to remove the temperature dependency from the data before any further analysis.

To remove the temperature dependency from the data of the geomagnetically storm day, a temperature compensation technique was applied by removing average GICs of geomagnetically quiet days from the geomagnetically storm day approximated to have the same average daily temperature. Applying the temperature compensation technique resulted in good correlation between measured and modelled results during periods of rapid fluctuations compared to periods of slow fluctuations. The differences in the results can be attributed to the approximations made for the temperature compensation technique. In addition, another investigation was performed which involved removing 1.3 A constant offset

from the measured data after applying a temperature compensation technique. This resulted in good correlation during periods of slow fluctuations and worsened the correlation during periods of rapid fluctuations. The offset was attributed to the differences in the temperature of the geomagnetically quiet days and the geomagnetically storm day.

Other factors which could explain the difference between measured and modelled results can be attributed to the assumptions made in the calculation which used uniform plane wave method, uniform ground conductivity method and well as assumptions made about the frequency components of the resistance in the network which was neglected.

Looking at the exposure of the entire Namibian network using the magnetic data for the 2nd October, it was found that Ruacana had the highest GIC magnitude followed by Kokerboom, Auas and Obib substation. The remaining substations showed GIC maximums of less than 3 A.

An interesting observation was found indicating a variation in the 1-4 Hz band of the neutral current for both quiet days and stormy days.

Another investigation was performed to find out if there is a capacitive current present in the neutral. This investigation was inconclusive due to the inconsistencies in the data of the current phases and phase voltages.

Chapter 7

Conclusion

7.1 Properties of the Namibian transmission network making it susceptible to GICs

From literature it was found that the Namibian transmission network is characterised to consist of long transmission lines and low ground conductivity making it susceptible to GICs. The highest published GIC magnitude obtained for the Namibian network was 30 A at the Ruacana substation on the 2002 network using the 13th March 1989 solar storm. It was also found that south-northerly lines, such as the Ruacana-Omburu line, appear to be more susceptible to GICs. This could be one of the reasons for the high GIC magnitude at the Ruacana substation.

7.2 Validation of the Nodal Admittance method using previous data

The Nodal Admittance method was proposed for GIC calculations in this dissertation due to its flexibility to use non-uniform electric field for each region in the network as well as ease of use compared to the *a&b* parameter method which only accepts uniform electric field. The Nodal Admittance method was first tested against previously published data using the *a&b* parameter method. This was done as a first validation process for the Nodal Admittance method. Previously published results obtained using the *a&b* parameter method were compared with those obtained using the Nodal Admittance method, under similar conditions, and good agreement. After validating the Nodal Admittance method using published results, the next step is to take measurements to further validate the calculation technique.

7.3 GIC measurement equipment and field installations

The proposed GIC measurement devices included the use of Hall-effect transducers to measure phase currents and voltages as well as the neutral current. This was done using VT's, AC-DC converters as a power source for the Hall-effect transducers, voltage and current modules and the National Instrument (NI) data logger. The complete equipment set-up was tested successfully in the laboratory before installations in the transmission network using a published laboratory set-up.

Based on past modelled results obtained using past solar storms, substation connectivity, substations location and historical events, two sites were chosen for GIC installations namely Ruacana and Obib substation. After rigorous tests were performed at the two substations, to ensure that the readings from the data logger were reliable using various methods, the installations at the two sites were completed successfully. It was later observed that the Ruacana measurements were not consistent and only the Obib measurements were used in the analysis for this dissertation. An investigation of the Ruacana installations will be performed outside the scope of this dissertation. Moreover, the voltage measurements at the Obib substation were found to be heavily distorted making the data unreliable and were also omitted in the analysis.

7.4 Measurement results

During preliminary analysis of the data for the Ruacana substation, it was found that there was a significant current of magnitude higher than 6 A flowing in the neutral conductor, even when the transformers were offline and isolated from the network. As a result, the Ruacana readings were found to be inconsistent and were omitted in this dissertation. Moreover, outside the scope of this dissertation, the Ruacana installation will be investigated and revised to ensure that the measurements are reliable for future analysis.

From the Obib readings, after applying an FFT analysis on the neutral current data, it was found that there was a significant un-balance and a dominant 1st harmonic of magnitudes as high as 6 A AC with a significant 3rd harmonic. The presence of the AC current in the neutral was attributed to the un-transposed transmission line feeding the Obib substation. Furthermore, an analysis was done to investigate whether the presence of the dominant 1st harmonic in the neutral current data is a result of the capacitive current presence. This investigation was not conclusive because of the inconsistencies found in the phase currents since a high zero offset was observed in the phase current measurements making it unreliable for phase shift analysis.

The entire period from July to September 2013 was regarded as solar quiet days since no CME was reported during this period. The only strong geomagnetic storm reported took place on the 2nd October 2013. All the days prior to the 2nd October were regarded as geomagnetically quiet days and only the 2nd October was regarded as a solar storm day. A 1-minute average was performed on the neutral current data to remove high frequency components leaving only the “quasi” DC components which are referred to as GICs. It was found that the results of the geomagnetically quiet days showed a similar trend as that of the diurnal temperature variation. The trend remained constant from 00:00 to 08:00 and

increased between 8:00 and 20:00 and thereafter it remained constant until 12:00 the following day. From geomagnetically quiet days, it was inconclusive as to how much GICs was flowing in the network which posed a need to analyse data of corresponding to a geomagnetically storm day due to a highly diurnal temperature variation observed.

A CME took place on the 2nd October 2013 indicated by K (HER) -7 index. A significant variation in the 1-minute average neutral currents was observed in the results of the geomagnetically storm day in comparison to that of geomagnetically quiet days. From geomagnetically quiet day's results, it was noticeable that the neutral current data might be highly influenced by the daily temperature variations since the measurements are taken outdoors. For this reason, a direct comparison of the measured results with the modelled results might not give an accurate representation of the magnetically quiet day's results. Consequently, to be able to compare the measured results with the modelled results, a temperature compensation technique was applied to the measured results to remove the diurnal temperature effects from the readings.

Applying a temperature compensation technique to the measured data of the geomagnetically storm day resulted in good correlation with the modelled data during periods of rapid fluctuations compared to periods of slow fluctuations. To further investigate the temperature compensation technique and improve the correlation of the results, a 1.3 A offset was removed from the measured data and this resulted in good correlation during periods of slow fluctuations but worsened the results during periods of rapid fluctuations. Further investigations are necessary regarding temperature compensation techniques and the equipment calibration to analyse the measurement results and improve the correlation with modelled results.

Moreover, an analysis was done to investigate the presence of variations in the 1-4 Hz band of the neutral current data. It was observed that there were fluctuations in the 1-4 Hz band for both the magnetically quiet days and magnetically storm day. Further research is needed to investigate this characteristic if it is unique to the Namibian transmission network or what properties of the network may cause this characteristic.

7.5 Exposure of the Namibian transmission network

To investigate the exposure of the network under magnetically storm conditions, the magnetic field data for the 2nd October 2013 obtained from the Keetmanshoop magnetic observatory were used for the entire network. Thereafter, the Nodal Admittance method was used to calculate GICs in the network assuming constant electric field and uniform ground conductivity with M=10. It was found that Ruacana had the highest GIC magnitude followed

by Kokerboom, Auas and Obib substation. The remaining substations showed GIC maximums of less than 3 A. These magnitudes could be large if the CME was categorised above K(HER)=7 index and there might be a need to investigate what happened when the network is exposed to such high current magnitudes. High GIC magnitudes may drive transformers into half-cycle saturation which may result in increased non-active power and overheating which could lead to transformer winding damages. Transformers under half-cycle saturation could also lead to increased harmonic content which may affect protective devices leading to improper tripping and in extreme cases it may lead to disruption of power or blackouts.

Meanwhile, the Namibian transmission network is currently undergoing extensions and plans are still being made for extensions. Consequently, there is a need to first investigate how these extensions will affect GIC exposure of each individual substation. Since the CME recorded during the course of the measurements resulted in a geomagnetic storm with K(HER)=7 index and resulted in GICs of 30 A flowing at the Ruacana substation, high GIC magnitudes can be expected to flow if the network is exposed to a geomagnetic storm with K(HER)>7. To avoid possible power disruption during large solar storms, there might be a need adopt mitigation techniques as described in chapter one. Further investigations are needed to understand the extent to which mitigation techniques will be deployed in the NamPower network and the threshold necessary to activate the mitigation techniques.

7.6 Monitoring of GICs

The Namibian transmission network span over a large area and it is recommended that to be able to improve the accuracy between measured and modelled results, there is a need to extend GIC measurement network to substations located further apart to see how this impacts the correlation of the results for individual substations. It is also useful to increase the number of magnetic observatories to be able derive a non-uniform electric field for the network. Care should be taken when installing measurement devices to make sure the measurements are reliable and can be used to investigate additional characteristics of the network such as to calculate power factor in the presence of GICs.

7.7 Testing of the hypothesis

The hypothesis set out in chapter one was that advanced network modelling algorithms can be used efficiently together with measurement results, to predict the flow of GICs in the Namibian transmission network. In an attempt to test the validity of this hypothesis, six research questions were posed. The first three questions were: what appropriate ground

conductivity, simulation techniques and parameters needed for the calculation technique can be used for the Namibian network. To answer these questions, several calculation techniques were found in literature namely plane wave method, SECS method and Complex Image Method (CIM). These techniques can be used with either uniform ground conductivity or 3-D ground conductivity model to calculate the electric field induced in the ground as a result of the fluctuations of the earth magnetic field.

The calculation of GICs flowing in the network can either be done using the *a&b* parameter method or the Nodal Admittance method. The Nodal Admittance method was proposed for this dissertation and tested using published data obtained from a previous study which used the *a&b* parameter method under the same conditions and good agreement was found. The Nodal Admittance method was preferred over the *a&b* parameter method due to its ease of use as well as flexibility to adopt the use of non-uniform electric field data for the network. Further validation of the Nodal Admittance technique was done using measurements.

The next two research questions were: how will GIC measurements be done and how accurately the modelled results compare with measured results. In an attempt to answer these two questions, two measurement techniques were found in literature namely directly measuring GICs in the transformer neutral and the indirect method whereby the magnetic field induced under the transmission line due to the GICs flowing in the line is measured. The direct method was proposed for this dissertation to further validate the Nodal Admittance method due to its simplicity.

Measurement devices proposed for GIC measurements were chosen and the criteria for choosing them were discussed. The proposed measurement technique was then tested successfully on a published laboratory set-up and later installed in the network at the two proposed substations namely; Ruacana and Obib substation. This was done to be able to compare measured results with modelled results obtained using the Nodal Admittance method.

The Nodal Admittance method was used to simulate GICs in the Namibian network. Measured results of geomagnetically quiet days were observed to be highly dependent on daily temperature variation. As a result, results obtained for the geomagnetically storm day (2nd October) were also regarded to be temperature dependent. Consequently, a temperature compensation technique was applied on the geomagnetically storm day results and good agreement was observed between the modelled and measured results during periods of rapid fluctuations compared to slow fluctuations. Furthermore, a 1.3 A offset was observed between measured and modelled results of the geomagnetically storm day after the temperature compensation technique was applied. This offset was attributed to a

possible temperature difference between the geomagnetically quiet days and the geomagnetically storm day. Removing the 1.3 A offset resulted in good correlations during periods of slow fluctuations compared to periods of rapid fluctuations as observed when only the temperature compensation was applied.

Testing of the hypothesis was not fully conclusive because there were some problems with temperature compensations and calibrations of the measurement devices. Therefore, it is not possible to validate the hypothesis. However, it is clear that the measurements respond in a very similar way to what would be expected. After calibration and temperature compensation concerns have been attended to, there would be measurement figures which can be used to calibrate the modelled results and make up for the unknown parameters in the calculation technique such as ground conductivity.

References

Amuanyena L.A.T, Gaunt, C.T, *Effects of geomagnetically induced currents (GICs) on power transformers and reactors,* SAUPEC, 2003

Arinmez I.A., *Managing the impact of geomagnetically induced currents on the NGC transmission system*, in Proc. Of 2001 Winter Meeting of the IEEE Power Engineering Society, Vol 1, pp. 336 28 January-1 February 2001

Bachinger F., Hackl A., Hamberger P., Leikermoser A., Leber G., Passath.,Stpessl M., *Direct current in transformers: effects ad compensation*, A2-301, Cigre, Paris, France, 26-31 August 2012

Bernhardi E.H, Tjimbandi T.A, Cilliers P.J, Gaunt C.T, *Improved calculations of geomagnetically induced currents in power networks in low-latitude regions*, PSCC, Glasgow, 2008

Bernhardi E.H, *Modelling geomagnetically induced currents in Southern Africa*, BSc(Hons) project report, NASSP, University of Cape Town, 2006

Boteler D.H., *Geomagnetic hazards to conducting networks*, Kluwer Academic Publishers, Netherlands, Natural hazards, 28: 537-561, 2003

Boteler D.H., Pirjola R.J., *Modelling geomagnetically induced currents produced by realistic and uniform electric fields*, IEEE Transaction on Power Delivery, Vol.13, No.4, October 1998

Boteler D.H., Bui-Van Q., Lemay J., *Directional sensitivity to geomagnetically induced currents of the Hydro-Quebec 735 kV power system,* IEEE Transactions on Power Delivery Vol. 9, No. 4, October 1994

Bolduc L., *GIC observations and studies in the Hydro-Quebec power system*, Journal Atmos. Sol. Terr. Phys. 64, 1793-1802, 2002

Breckenridge T.H., Cumming T., Merron J., *Geomagnetic induced current detection and monitoring*, Seventh International Conference on IEEE, pp. 250-253, 2001

Chisepo K.H, Gaunt C.T Oyedokun D.T., *Testing the response of laboratory bench transformers to geomagnetically induced like currents,* Southern Africa Universities' Power Engineering Conference (SAUPEC) 2013, Potchefstroom, South Africa, 31 January-1 February 2013

Department of public utilities, *Reliability Factors Affecting Electric Infrastructure*, December 2008

Foss A., Boteler D.H., "*GIC simulation using network modeling"*, Canadian Conference on Electrical and Computer Engineering (CCECE), pp4, IEEE Canada, Ottawa, Canada, 7-10 May 2006

Gaunt C.T, Malengret M, *Why we use the term non-active power, and how it can be measured under non-ideal power supply conditions*, IEEE PES PowerAfrica Conference, Johannesburg, 2012

Gaunt C.T., Coetzee G., *Transformer failures in regions incorrectly considered to have low GIC-risk,* Paper no. 445, IEEE Power Tech, Lausanne, Switzerland, 1-5 July 2007

Girgis R., Gramm K., *Effects of Geomagnetically Induced Currents on Power Transformers and Power Systems*, A2-304, Cigre, Paris, France, 26-31 August 2012

House of Commons Defence Committee, *Developing Threats: Electro-Magnetic Pulses (EMP)*, Tenth Report of Session 2010–12

IEEE Transmission and Distribution Committee Working Group on Geomagnetic Disturbances and Power system effects, *Geomagnetic disturbances effect on power systems*, IEEE transaction on power delivery, Vol.8, No. 3, pp. 1206-16, July 1993

Kappenman J.G., Albertson, V.D., *Bracing for the geomagnetic storms,* IEEE Spectrum, pp.27-33, March 1990

Kenny R., *Detection of the presence of Geomagnetically induced currents*, BSc(Eng) Thesis, University of Cape Town, 2005

Koen, J., Gaunt, C.T., *Geomagnetically Induced Currents in the Southern African Electricity Transmission Network*, IEEE Bologna, PowerTech, vol.1, p7, NJ, USA, 2003

Koen J., *Geomagnetically induced currents and their presence in the Southern African electricity transmission network.* PhD Thesis, University of Cape Town, 2002

Lehtinen M., Pirjola R., *Currents produced in earthed conductor networks by geomagnetically-induced electric fields.* Annales Geophysicae, Vol. 3, No. 4, pp. 479-484, 1985

Liu C-M., Liu l-G., Yang Y., *Monitoring and Modeling geomagnetically induced currents in power grids of China*, IEEE, 2009

Molinski T.S, *Why Utilities respect geomagnetically induces currents*, Journal Atmospheric and Solar-Terrestrial Physics, Vol. 64, pp. 1765 – 1778, 2002.

Ngnegueu T., Marketos F., Devaux F., Xu T., Bardsley R., Barker S., Baldauf J., Oliveira J., *Behaviour of transformers under DC/GIC excitation: Phenomenon, Impact on design/design evaluation process and Modelling aspects in support of Design*, A2-303, Cigre, Paris, France, 26-31 August 2012

Ngwira C.M., Pulkkinen A., McKinnell L.A., Cilliers P.J., *Improved modelling of geomagnetically induced currents in the South African power network,*Space Weather, 6, S11004, 2008

Ngwira, C.M., McKinnell L.A., Cilliers P.J., Viljanen A., Pirjola R., *Limitations of the modelling of geomagnetically induced currents in South African power network*, Space weather, Vol. 7, S10002, 2009

Ngwira, C.M., McKinnell L.A., Cilliers P.J., *Geomagnetic activity indicators for geomagnetically induced current studies in South Africa*, ELSEVIER, 2011

Oyedokun D.T, M.N Simon, C.T Gaunt, *Introduction of a more detailed calculation of Geomagnetically Induced Currents in transmission networks*, Southern Africa Universities' Power Engineering Conference (SAUPEC) 2013, Potchefstroom, South Africa, 31 January-1 February 2013

Pinto L.M.V.G., Szczupak J., Drummond M.A., Macedo L.H., Barreto L.M., *Geomagnetically Induced Currents: The Ultimate Threat to System Security*, PowerTech, Russia, June 2005

Pirjola R.J., *Fundamental about the flow of geomagnetically induced currents in a power system applicable to estimating space weather risks and designing remedies*, Journal of Atmospheric and Solar-Terrestrial Physics, No. 64, pp. 1967-1972, 2002

Pirjola R.J., *Effects of space weather on high-latitude ground system*, Finnish Meteorological Institute, Geophysical research division, February 2005

Pirjola R.J., Boteler D.H., *Geomagnetically induced currents in European high-voltage power systems*, IEEE Ottawa, May 2006

Pirjola R.J, Liu C., Liu L., *Geomagnetically induced currents in Electric power transmission networks at different latitudes*, IEEE Beijing China, 12-16 April 2010

Pirjola R.J, Viljanen A., *Complex image method for calculating electric and magnetic fields produced by an auroral electrojet of a finite length*, Annales Geophysicae, Vol.16, pp 1434-1444, 1998

Prabhakara F.S., Hannett L.N., Ringlee R.J. Ponder J.Z., *Geomagnetic effects modelling for the PJM interconnection system Part II – Geomagnetically induced current study results,* IEEE Trans, on Power systems, PWRS, Vol. 7, No. 2,pp. 1239-1245, May 1992

Shepherd S.G., Shubitidze F., *Method of auxiliary sources for calculating the magnetic and electric fields induced in a layered Earth*, Journal of Atmospheric and Solar-Terrestrial Physics. Vol. 65, pp. 1151-1160, 2003

Simon M.N., Oyedokun D.T., Gaunt C.T., *Calculations of Geomagnetically Induces Currents (GICs) in the Namibian transmission network*, Southern Africa Universities' Power Engineering Conference (SAUPEC) 2013, Potchefstroom, South Africa, 31 January to 1 February 2013

Tjimbandi T.A., *Geomagnetically induced currents in South Africa*, BSc(Eng) Thesis, University of Cape Town

Trichtchenko, A. A., Boteler D. H., Foss A., *GIC modelling for an overdetermined system*, Canadian Conference on Electrical and Computer Engineering (CCECE),IEEE Canada, Ottawa, Canada, 7–10 May 2006

Viljanen A., Pirjola R., *Geomagnetically Induced Currents in the Finnish high-voltage power system, a geographysical review,* Surveys in Geophysics *15 (4), 383-408, 26 January 1994*

Viljanen A., Pirjola R., *Statistics on geomagnetically-induced currents in the Finish 400 kV power system based on recordings of geomagnetic variations,* Journal of Geomagnetism and Geoelectricity, Vol. 41, pp. 411-420, 1989

Viljanen A., Pulkkinen A., Amm O., Pirjola R., Korja T., and Bear Working Group, *Fast computational of the geoelectric field using the method of elementary current systems and planar Earth models*, Annales Geophysicae, pp. 101 -113, 1 January 2004

Watari S., Kunitake M., Kitamura K, Hori T.,Kikuchi T, Shiokawa K., Nishitani N.,Kataoka Y.,Kamide T., Watanabe Y., TsunetaY.,*Measurements of geomagnetically induced current in a power grid in Hokkaido, Japan,* SPACE WETHER, VOL. 7, no. 3, 2009

Wells L., Jeffery T., LABVIEW for everyone, Prentice-Hall, New Jersey, 1996

Zatjirua T., *Investigation of Geomagnetically induced currents in the transmission network of Namibia. BSc(Eng) Thesis,* University of Cape Town, 2005

Appendix

Namibian Transmission substation and line parameters

Substation number	2012 Namibian transmission substations
1	Aggeneis
2	Aries
3	Kokerboom
4	Ruacana
5	Omburu
6	Auas
7	Van Eck
8	Khan
9	Trekkopje
10	Rossing
11	Walmund
12	Kuiseb
13	Gerus
14	Otjikoto
15	Osona
16	Hardap
17	Obib
18	Karas
19	Harib

20	Oranjemond

From Substation	To Substation	Line admittance	Length [km]
1	20	0.33557	130
1	19	0.0997	109.06
1	19	0.0997	109.06
1	2	0.662252	196
2	3	0.362319	420
3	18	0.066724	163
3	18	0.066724	163
3	17	0.2157	252.9
3	16	0.0546	199
3	16	0.0546	199
3	6	0.1223	445.8
18	19	0.14709	73.94
18	19	0.14709	73.94
6	16	0.04258	255.4
6	16	0.04258	255.4
6	7	0.31989	34
6	7	0.31989	34
6	7	0.31989	34
7	12	0.062794	267.15

7	15	0.19148	58.56
7	5	0.1923	163
15	5	0.1075	104.3
13	5	0.08032	139.6
13	14	0.06422	174.6
12	11	1.0099	16.61
11	10	0.21237	52.8
10	8	0.254271	44.1
8	9	0.311245	53.9
8	5	0.0987	113.6
8	5	0.147677	113.6
4	5	0.1552	521.506

Substations single line diagrams

Ruacana substation single line diagram

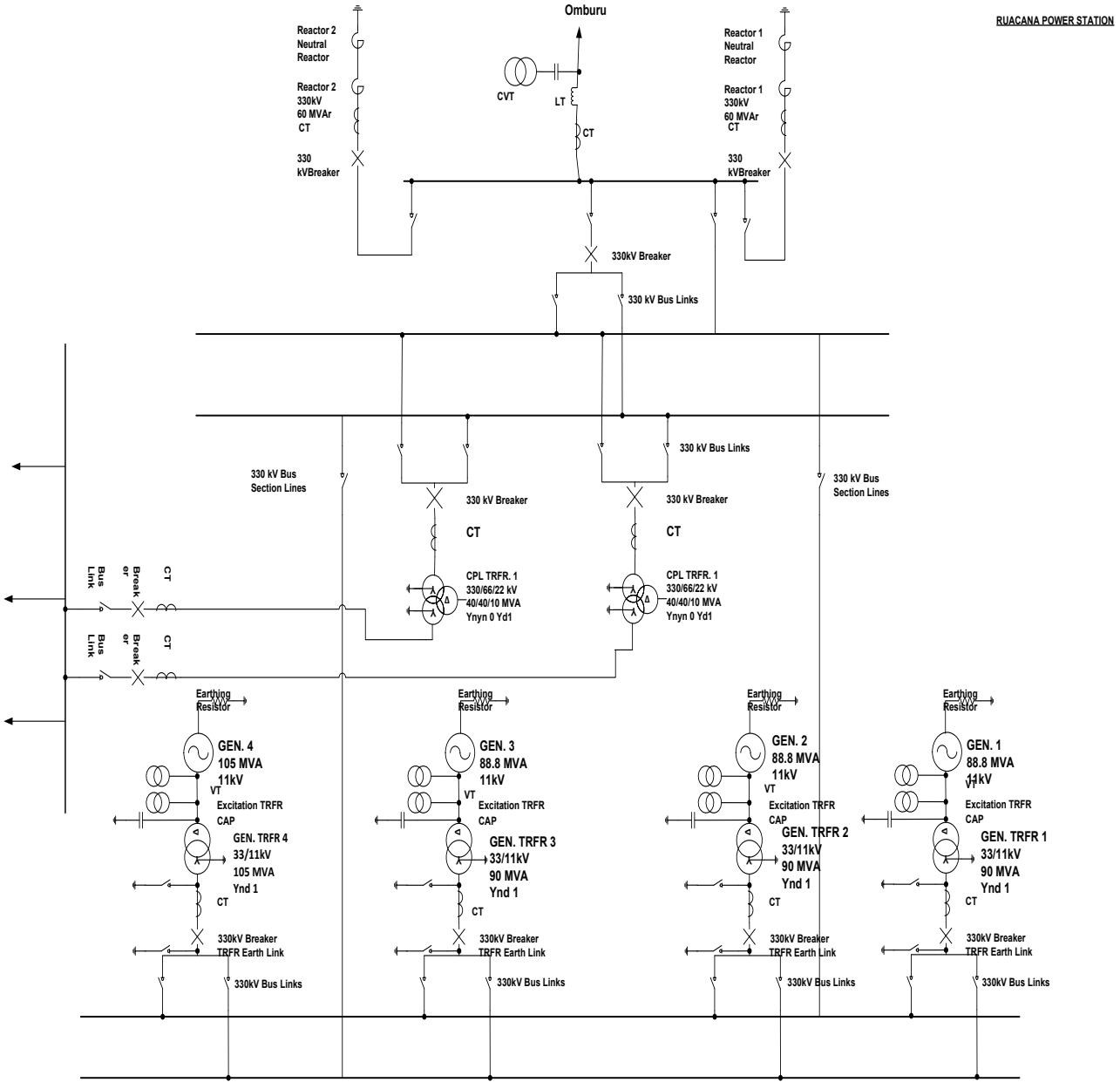

Obib substation single line diagram

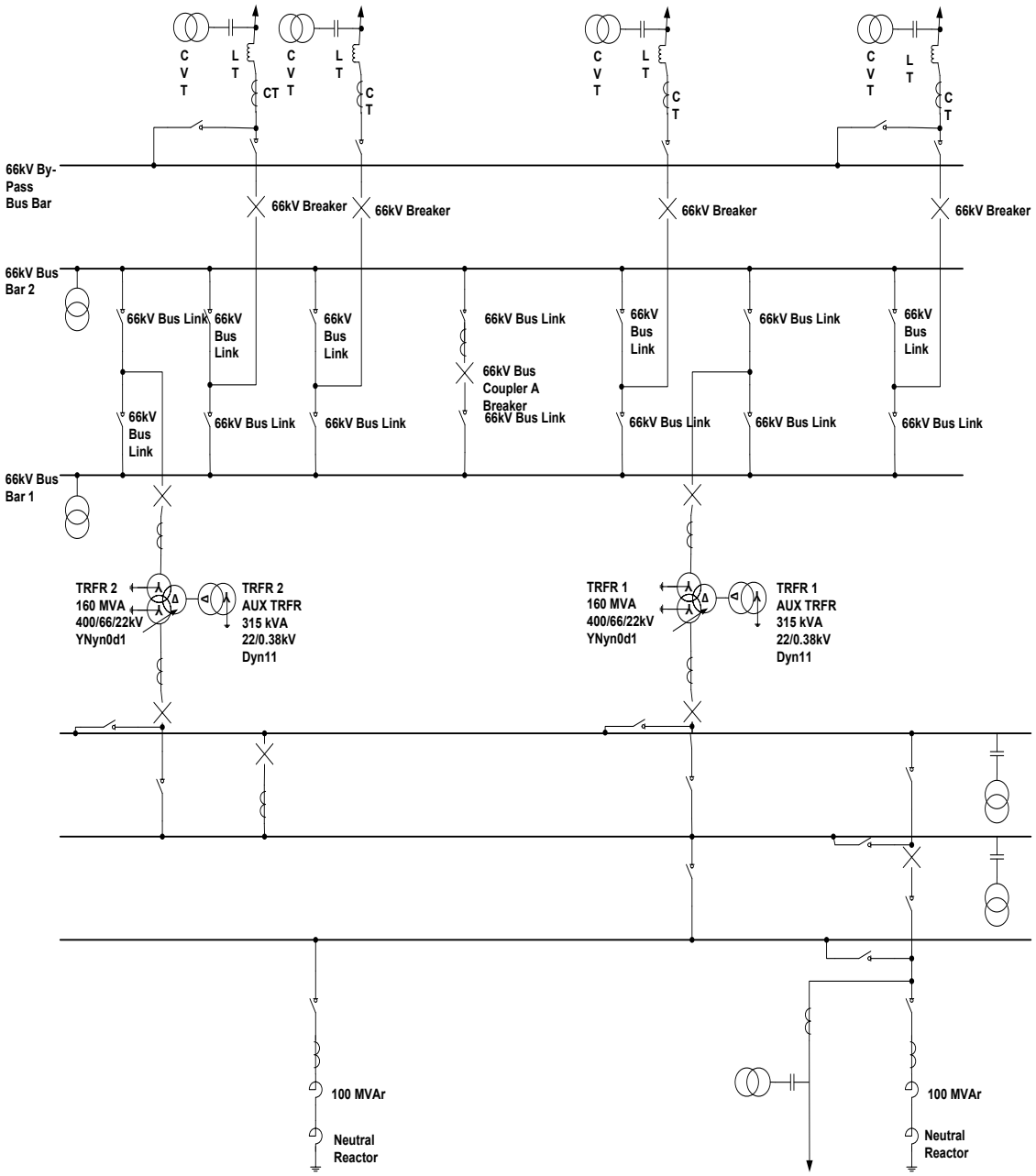

Abbreviations

CIM-Complex Image Method

CT-Current Transformers

CME- Coronal Mass Ejection

GIC-Geomagnetically Induced Current

DGA-Dissolve Gas Analysis

FFT-Fast Fourier Transform

GMD- Geomagnetic Disturbances

K (HER)-Local K-Index derived from the data recorded at Hermanus

KCL-Kirchhoff's Current Law

LABVIEW-Laboratory Virtual Instrumentation Engineering Workbench

NamPower- Namibian Power Utility

NI-National Instruments

P-Power

S-Active Power

SANSA-South African National Space Agency

SECS-Spherical Elementary Current Systems

VI- Virtual Instruments

VT-Voltage Transformers